Inorganic Chemistry

Article

pubs.acs.org/IC

Enhanced Catalytic Activity of Iridium(III) Complexes by Facile Modification of C,N-Bidentate Chelating Pyridylideneamide Ligands

Miquel Navarro,[†] Christene A. Smith,[†,‡] and Martin Albrecht*[,†]

[†]Department of Chemistry and Biochemistry, University of Bern, Freiestrasse 3, CH-3012 Bern, Switzerland

Supporting Information

ABSTRACT: A set of aryl-substituted pyridylideneamide (PYA) ligands with variable donor properties owing to a pronounced zwitterionic and a neutral diene-type resonance structure were used as electronically flexible ligands at a pentamethylcyclopentadienyl (Cp*) iridium center. The straightforward synthesis of this type of ligand allows for an easy incorporation of donor substituents such as methoxy groups in different positions of the phenyl ring of the C,N-bidentate chelating PYA. These modifications considerably enhance the catalytic activity of the coordinated iridium center toward the catalytic aerobic transfer hydrogenation of carbonyls and imines as well as the hydrosilylation of phenylacetylene. Moreover, these PYA iridium complexes catalyze the base-free transfer hydrogenation of aldehydes, and to a lesser extent also of ketones. Under standard transfer hydrogenation conditions including base, aldehydes are rapidly oxidized to carboxylic acids rather than reduced to the corresponding alcohol, as is observed under base-free conditions.

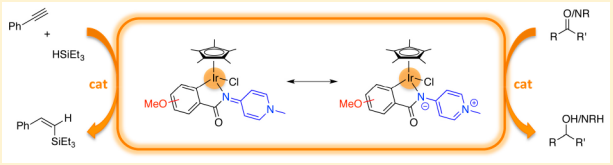

INTRODUCTION

Classic spectator ligands like phosphines, amines, or halides typically feature static bonding characteristics such as π-donor or π-acceptor properties, which can be more or less pronounced depending on the metal center to which they are coordinating. Such ligands traditionally stabilize a specific metal configuration; e.g., strong π acceptors preferably bind to low-valent, electron-rich metal centers.[1] More recently, non-innocent ligands that can significantly modulate their donor properties have become increasingly popular as a powerful class of ligands for a variety of homogeneous catalytic applications because the modular ligation alleviates the constrain of static ligands, which stabilize predominantly one specific configuration.[2] For example, Shvo's cyclopentadienone system or Noyori's diamine ligand can change from L-type neutral coordination to anionic X-type metal bonding during a catalytic cycle.[3] Similar L/X-type ambiguous ligand systems have been developed based on pyridines, guanidines, and related functional groups.[4] This ligand flexibility allows for facilitating *both* oxidative addition and reductive elimination processes on a putative catalytic cycle, properties that are highly attractive for the design of efficient catalysts, and offering opportunities also for materials science. Such dynamic bonding may, in fact, be one of the key features of N-heterocyclic carbenes (NHCs) that underpins their beneficial role in homogeneous catalysis through adoption of either a more neutral carbenic bonding (L-type) or a zwitterionic (X-type) bonding mode during catalytic transformations.[5−7]

Similar to NHCs, pyridylideneamines (PYEs) and pyridylideneamides (PYAs) are electronically highly flexible nitrogen-donor sites that can coordinate to the metal center as a π-acidic imine or as a π-basic pyridinium amide (Figure 1). Their electronic flexibility is represented by the two limiting resonance forms comprised of a diene heterocycle and a neutral imine donor site with minimal charge separation (**A**) and a zwitterionic form (**B**) that features an anionic amide donor site and aromatic stabilization of the pyridinium residue.[8] PYA coordination to transition metals has been pioneered by Johnson and Douthwaite,[9] and we have recently demonstrated the adaptiveness of PYAs in response to the external environment such as the solvent polarity.[10] Complexes with PYA or PYE ligands have shown high catalytic activity in different redox transformations including C−F bond activation,[9a] C−H bond stannylation,[11] water oxidation,[10b] and transfer hydrogenation,[10a,12] which warrants further investigation of PYAs as ancillary ligands to catalytically active metal centers.

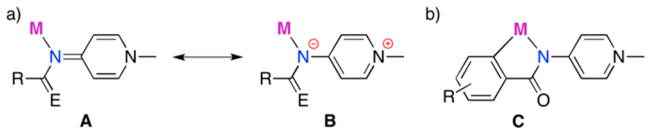

Figure 1. (a) Generic representation of PYE (E = H_2) and PYA (E = O) and their limiting neutral (**A**) and zwitterionic (**B**) resonance structures. (b) PYA ligand containing a chelating aryl group (**C**).

A major advantage of PYA ligands is their straightforward synthesis, which allows modifications to be introduced easily for fine-tuning the electronic and steric properties as a method to improve the catalytic activity.[13] Here, we applied this concept for facile catalyst tailoring by incorporating donor substituents in different positions of the phenyl ring of the C,N-bidentate chelating PYA ligand **C** (Figure 1). These modifications greatly enhance the catalytic activity of the coordinated iridium center.

Received: June 28, 2017

DOI: 10.1021/acs.inorgchem.7b01654
Inorg. Chem. XXXX, XXX, XXX−XXX

Scheme 1. Synthesis of the IrCp*PYA-Type Complexes

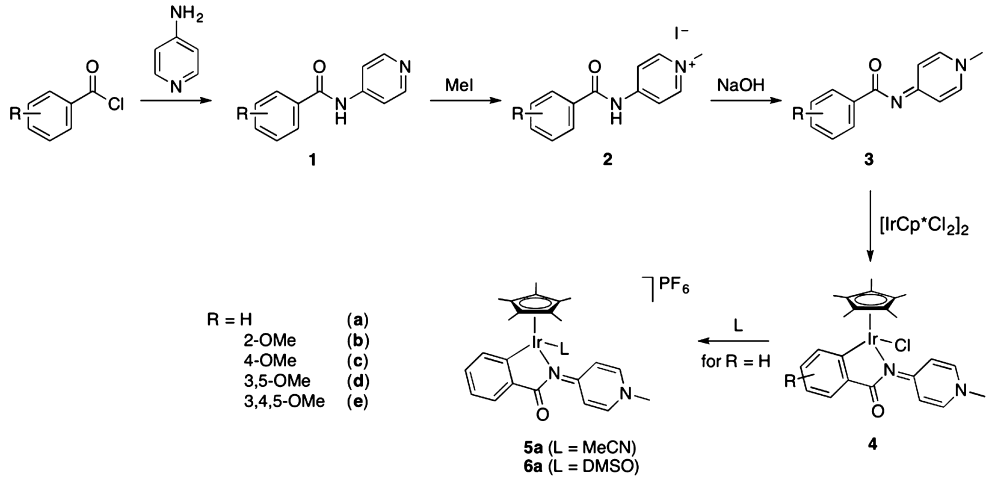

Table 1. Selected Bond Lengths (Å) and Angles (deg) of the IrPYA Complexes 4

	4a[a]	4b[b]	4c	4d	4e
Ir−C	2.045(2)	2.033(4)	2.053(7)	2.055(17)	2.047(3)
Ir−N	2.120(2)	2.095(3)	2.119(6)	2.096(14)	2.122(2)
average C_α−C_β	1.371(5)	1.366(13)	1.356(14)	1.38(3)	1.366(6)
average C_β−C_γ	1.410(5)	1.407(12)	1.416(14)	1.40(3)	1.407(6)
Ir−Cp $_{centroid}$	1.8316(11)	1.827(4)	1.829(3)	1.826(8)	1.8221(12)
C−Ir−N	78.12(9)	77.89(16)	78.0(3)	76.6(6)	77.73(10)
C−Ir−Cl	89.59(7)	89.92(12)	89.9(2)	87.5(5)	89.65(8)
N−Ir−Cl	85.67(6)	87.61(10)	86.07(17)	87.3(4)	89.48(7)

[a]Data from ref 10b. [b]Data for one of the two independent molecules in the unit cell; the average C_α−C_β and C_β−C_γ were calculated from both molecules.

RESULTS AND DISCUSSION

Synthesis. A set of PYA iridium complexes were prepared starting from differently substituted benzoyl chlorides in four straightforward synthetic steps (Scheme 1).[10b] Accordingly, benzoyl chlorides with one, two, or three aromatic OMe substituents were reacted with 4-aminopyridine to yield the corresponding amides **1a**−**1e**. Formation of the products was indicated by the diagnostic low-field singlet around 10.5 ppm in the ^{1}H NMR spectrum due to the amide NH proton. Subsequent alkylation with MeI occurred selectively and exclusively at the pyridine nitrogen, even in the presence of a large excess of alkylating agent, and afforded the pyridinium amide salt **2** in excellent yield.[14] All salts showed the characteristic $[M - I]^+$ signal in high-resolution mass spectrometry (HR-MS). Alkylation was further supported by ^{1}H NMR spectroscopy, which revealed a new singlet for the NCH_3 group (δ_H = 4.2) as well as a 0.3 to 0.5 ppm downfield shift of the pyridinium proton signals compared to the analogous resonances of the neutral pyridine resonances in **1**. Amide deprotonation was accomplished with simple bases such as NaOH in a straightforward CH_2Cl_2/H_2O extraction and afforded the free ligands **3a**−**3e** in good yield (64−84%). In addition to the disappearance of the amide proton, the ^{1}H NMR spectra of the free-base complexes also revealed a substantial upfield shift of about 0.8 ppm for the heterocyclic proton resonances.[8] In contrast, the aryl proton signals are barely affected, indicating that the pyridylidene system is involved in stabilizing the amide but not the (methoxy)aryl unit. Moreover, the heterocyclic proton shifts are identical in all compounds **3a**−**3e** and hence independent of, and electronically decoupled from, the aryl substitution pattern. The free bases are stable toward air and moisture and have been characterized also by elemental analysis.

The reaction of the free ligands with $[IrCp^*Cl_2]_2$ in the presence of NaOAc as an auxiliary ligand[15] induced cyclometalation and afforded the iridium complexes **4a**−**4e** in good yield (70−78%) as air-stable complexes that were purified by standard column chromatography on silica. Cyclometalation was confirmed for all complexes by the loss of one proton signal in the aromatic region of the ^{1}H NMR spectrum. Moreover, the *m*-OCH_3 groups in **4d** and **4e** appeared as two distinct singlets due to the reduced symmetry upon cyclometalation.[16] The ^{13}C resonance of the amide carbonyl appeared at lower field than that in the precursor compound, in agreement with coordination of the amide to the metal center.[17] While the methyl group of the Cp* ligand resonates at almost identical frequency in all five complexes [δ_H = 1.50 (±2); δ_C = 9.2 (±1)], the ring carbon resonances are deshielded if the aryl ring contains methoxy substituents (δ_{Cp} = 82.3 for complex **4a** versus 87.4 (±2) for complexes **4b**−**4e**). This difference suggests a direct electronic influence of the aromatic substituents on the electronic configuration of the IrCp* unit.

The structures of all complexes were unequivocally confirmed by single-crystal X-ray diffraction analysis. The molecular structures show the classical three-legged piano-stool geometry with the iridium center in a pseudotetrahedral geometry. Bond lengths and angles around the iridium center

DOI: 10.1021/acs.inorgchem.7b01654
Inorg. Chem. XXXX, XXX, XXX−XXX

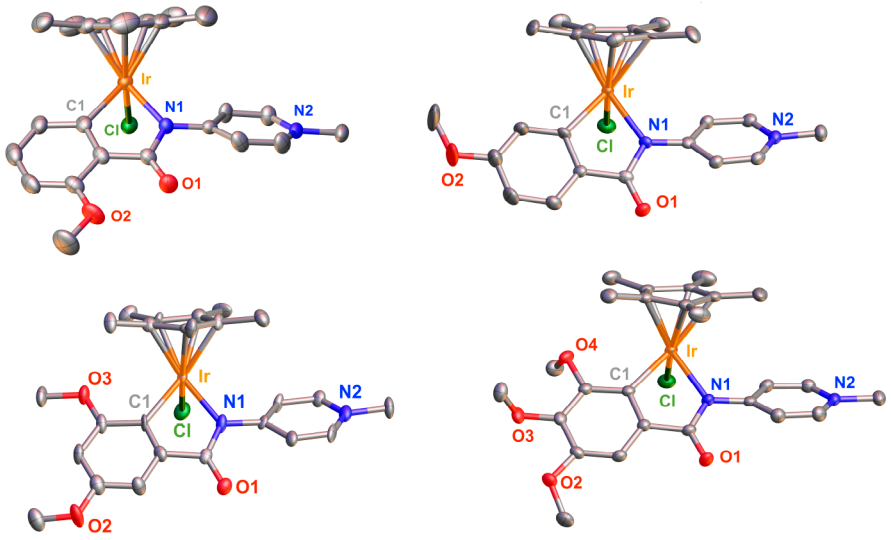

Figure 2. ORTEP representation of complexes **4b**–**4e** (50% probability; hydrogen atoms and cocrystallized solvent molecules omitted for clarity).

are identical within standard deviations for all complexes (Table 1). We note that the pyridyl C_α–C_β bonds are consistently shorter (average 1.37 Å) compared to the C_β–C_γ bonds (1.41 Å), confirming considerable contribution of the neutral diene-type resonance structure in the solid state (cf. Figure 2), in agreement with previous studies.[10,12] The essentially identical C_α–C_β bond distances for all five complexes corroborate the conclusions deduced from NMR spectroscopy that the aryl substitution pattern does not perturb the electronic configuration of the heterocycle. This disconnection is remarkable because the electron-donating properties of the methoxy groups are expected to enhance the electron density at the iridium center and hence enhance the iridium-to-imine back-bonding. Such interactions would favor the contribution of diene-type resonance structures with increasing numbers of methoxy substituents. However, no such trend is indicated by the data for complexes **4a**–**4e**, and the diene structure is equally pronounced, e.g., for complexes **4b** and **4e** containing one and three OMe substituents, respectively.

Closer inspection of the bonding situation around the iridium-bound nitrogen nucleus indicates a dihedral angle of about 35° between the pyridine heterocycle and the amide functionality [determined as the C_β–C_γ–N–C(=O) torsion angle, Table S1], which minimizes the overlap of the π electron density between these two systems. This tilting is in agreement with the negligible contribution of a zwitterionic form with an oxo anion, as deduced from IR data recorded on related complexes.[12] These data showed no perturbation of the NC(=O) amide unit upon solvent modification, while the pyridylidene amide moiety was strongly affected. The sum of the three bond angles around the iridium-bound nitrogen is exactly 360°, confirming sp^2 hybridization of this nucleus. The torsion angles between the carbonyl unit of the amide and the N–Ir bond are very close to 180°, while the torsion angle between the N–Ir bond and the pyridyl C_γ–C_β bond is very similar to the dihedral angle of the pyridyl ring with the N–C(=O) bond vector. These data indicate that, in the solid state, π electron overlap of the Ir–N bond is stronger with the carbonyl unit than with the pyridyl heterocycle, which is twisted out of the nitrogen sp^2 plane. As a consequence, the PYA ligand shows ambiguous characteristics: the partial C=C double-bond localization points to a significant contribution of the neutral resonance form (**A** in Figure 1), while bond and torsion angle analysis suggests a predominance of the resonance form **B** (Figure 1).

Catalytic Transfer Hydrogenation. The effect of ligand modification in these PYA ligands was probed in iridium-catalyzed transfer hydrogenation of ketones.[18] Initially, benzophenone was used as a model substrate to compare the activities of all of the complexes. Under standard transfer hydrogenation conditions using *i*PrOH as both the dihydrogen source and solvent and KOH as the base (100:10:1 substrate/base/catalyst), the unsubstituted complex **4a** displayed modest activity, reaching essentially full conversion within 24 h at 1 mol % loading (Table 2). This performance is a considerable improvement compared to that of $[IrCp^*Cl_2]_2$ as a benchmark complex, which only reached 39% conversion under identical conditions. No significant difference in the catalytic activity was observed upon exchange of the spectator ligand from an anionic chloride (**4a**) to neutral acetonitrile (MeCN; **5a**) or dimethyl sulfoxide (DMSO; **6a**; entries 1–3), suggesting that

Table 2. Transfer Hydrogenation of Benzophenone with PYA Iridium Complexes 4–6[a]

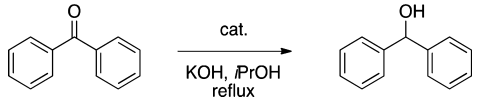

		conversion/%[b]		
entry	catalyst	2 h	4 h	24 h
1	**4a**	7	27	99
2	**5a**	4	28	99
3	**6a**	2	13	99
4	**4b**	77	99	n.d.
5	**4c**	30	96	99[c]
6	**4d**	93	99[d]	n.d.
7	**4e**	2	4	30
8	$[IrCp^*Cl_2]_2$	n.d.	n.d.	37

[a]General conditions: benzophenone (1.0 mmol), KOH (50 μL, 2 M in H_2O, 0.1 mmol), anisole (1.0 mmol), iridium complex (0.01 mmol), *i*PrOH (5 mL), reflux temperature. [b]Determined by ^1H NMR spectroscopy (error ±3%) with anisole as the internal standard; n.d. = not determined. [c]After 5 h. [d]After 3 h.

DOI: 10.1021/acs.inorgchem.7b01654
Inorg. Chem. XXXX, XXX, XXX–XXX

Table 3. Catalytic Transfer Hydrogenation of Different Ketones[a]

entry	substrate	product	yield (0.5 h) /%	time (>99% yield) /h
1		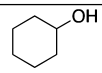	25	2
2	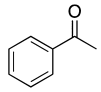	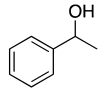	14	3
3	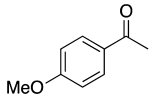	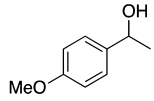	<5	4[b]
4	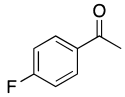	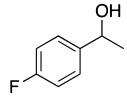	34	2
5	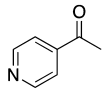	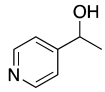	52	1
6	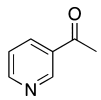	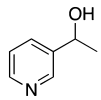	81	1
7	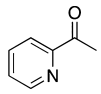	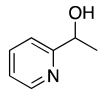	85	1

[a]General conditions: substrate (1.0 mmol), complex **4d** (0.01 mmol), KOH (50 μL, 2 M in H_2O, 0.1 mmol), anisole (1.0 mmol), *i*PrOH (5 mL), reflux temperature. Yields determined by ^1H NMR spectroscopy (error ±3%) with anisole as the internal standard. [b]65% yield.

the ancillary ligand is not bound to the metal center during the catalytic transformation. The lower conversion of complex **6a** at the initial stages of the reaction is probably due to the higher stability of the Ir−S_{DMSO} bond compared to the Ir−Cl and Ir−N_{MeCN} bonds in complexes **4a** and **5a**, respectively.[10b] The catalytic activity of the complex is markedly improved when electron-donating methoxy substituents are available on the ligand scaffold. Thus, complexes **4b** and **4c**, both containing one methoxy substituent, showed substantially higher catalytic activity and achieved full conversion in 4 and 5 h, respectively (entries 4 and 5). The incorporation of a second methoxy group enhances the catalytic activity even further, and complex **4d** reaches 93% conversion after 2 h and essentially full conversion within 3 h (entry 6), corresponding to about a 10-fold improvement of the catalytic activity compared to the parent complex **4a**.[19] While this trend suggests that an electron-rich iridium(III) center is beneficial for catalytic turnover, a subtle balance is operational. When a third methoxy group is added to the ligand as in complex **4e**, the catalytic activity does not increase further but drops even below the performance of the unsubstituted complex **4a** and reaches a low 30% conversion after 24 h (entry 7). This different behavior suggests that another step in the catalytic cycle is substantially affected by the presence of three substituents on the aryl ligand. The radical change in the activity of **4e** in comparison to that of **4b**−**4d** is surprising, and while we do not have mechanistic evidence to rationalize this activity change, an electronic effect seems unlikely.[20] Mesomeric stabilization does not appear to be particularly significant for controlling the catalytic activity because the activities of the complexes with methoxy substituents ortho/para or meta to the iridium center are very similar (**4d** vs **4b**). Likewise, inductive effects are not substantially altering the catalytic activity, as demonstrated by the moderate increase of activity upon the introduction of one versus two methoxy groups to the ligand scaffold. It is therefore difficult to conceive that electronic factors induced by the third methoxy group of **4e** lead to an almost complete shutdown of the catalytic activity. More likely, the presence of ortho-positioned methoxy groups influences the orientation of the OMe group ortho to the iridium-bound carbon. Therefore, we tentatively attribute the low activity of **4e** to a buttressing effect of the vicinal methoxy group,[21] which is caused by excessive substitution of the arene and which results in efficient shielding of the iridium coordination sphere. According to this model, the additional OMe substituent in **4e** compared to **4d** inhibits a flexible arrangement of the vicinal methoxy group and hence hinders substrate coordination, which significantly abates catalytic turnover. Irrespective of these mechanistic consequences, the different activities of complexes **4a**−**4e** and the poor activity of the PYA-free $[IrCp^*Cl_2]_2$ iridium complex (entry 8) underpin the efficacy of ligand aryl substitution as a methodology to tailor and optimize the catalytic activities of these PYA iridium complexes.

On the basis of its better catalytic activity, complex **4d** was used as the catalyst precursor for a set of different substrates (Table 3). Cyclohexanone as an aliphatic ketone was fully converted within 2 h (entry 1).[22] Likewise, acetophenone was transfer hydrogenated to 1-phenylethanol at a slightly slower rate and within 3 h. Aromatic substituents on acetophenone displayed the expected effect, with electron-withdrawing substituents increasing the electrophilicity of the carbonyl group and hence facilitating reduction, while electron-donating substituents had the opposite effect (entries 2−4).[18] Along these lines, transfer hydrogenation of acetylpyridine proceeded

DOI: 10.1021/acs.inorgchem.7b01654
Inorg. Chem. XXXX, XXX, XXX−XXX

significantly faster than that of (substituted) acetophenones and reached maximum conversion in just 1 h (entries 5−7). The conversion rate is dependent on the isomer, viz., 2-, 3-, or 4-acetylpyridine (see conversion at 0.5 h, entries 5−7); however, complete conversion at 1 h suggests a purely electronic role of the pyridyl unit in this reaction. In particular 2-acetylpyridine is for most catalysts a challenging target because both the substrate and the alcohol product are potentially chelating ligands that tend to poison the catalyst.[23] The smooth transformation of this substrate tentatively suggests the presence of only one labile coordination site at the iridium center in the catalytic species originating from these bidentate PYA complexes and therefore lends indirect support to the strong chelation of the PYA ligand.

Further mechanistic insight was gained from a transfer hydrogenation experiment in heptadeuterated *i*PrOH, $(CD_3)_2CDOH$, as a selective HD donor, and benzophenone as the acceptor. The diphenylmethanol obtained from this reaction was completely deuterated at the carbinol position with less than 5% hydrogen incorporation according to ^1H NMR spectroscopy. The selective transfer of the deuterium atom from the carbon site of the hydrogen donor (*i*PrOH-d_7) to the carbonyl carbon of the substrate is in agreement with a monohydride mechanism for the transfer hydrogenation reaction.[18b,24] This mechanism requires only one labile coordination site and therefore corroborates the model deduced above.

Because pyridyl moieties were tolerated by the catalytically active species without significant compromises of the turnover rates (cf. Table 3, entries 5−7), imines were investigated as substrates for transfer hydrogenation. The model substrate *N*-benzylideneaniline was almost fully hydrogenated to *N*-benzylaniline after 4 h using iridium complexes **4a**−**4e** under the same standard conditions (Table 4). The longer reaction

Table 4. Transfer Hydrogenation of *N*-Benzylideneaniline with PYA Iridium Complexes 4a−4e[a]

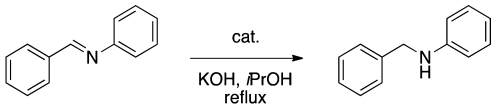

		conversion/%[b]		
entry	catalyst	1 h	2 h	4 h
1	**4a**	30	49	87
2	**4b**	34	54	94
3	**4c**	31	50	92
4	**4d**	31	48	86
5	**4e**	34	53	80

[a]General conditions: *N*-benzylideneaniline (1.0 mmol), KOH (50 μL, 2 M in H_2O, 0.1 mmol), hexamethylbenzene (1.0 mmol), iridium complex (0.01 mmol), *i*PrOH (5 mL), reflux temperature. [b]Determined by ^1H NMR spectroscopy (error ±3%) with hexamethylbenzene as the internal standard.

time required to reach quantitative yields is in line with the expected lower activity of imines compared to ketones.[22b,25] The catalytic activity for imine hydrogenation is not significantly affected by the different electronic properties of the PYA ligands, and all complexes display similar conversion rates (entries 1−5). However, catalysts **4b** and **4c**, both containing only one methoxy group, are slightly more active catalyst precursors and reach >90% conversion after 4 h (entries 2 and 3). We note that while the introduction of a third methoxy substituent on the aryl group deactivated the iridium center for catalytic ketone transfer hydrogenation, no such effect was observed for imine reduction, and complex **4e** performed equally well when compared with the related complexes **4a**−**4d** in imine transfer hydrogenation (entry 5).

On the basis of these catalyst screening results, the iridium complex **4b** was used as the catalyst precursor for transfer hydrogenation of different imines (Table 5). Functionalized imines showed the same trends as those established for ketones, with electron-withdrawing substituents accelerating hydrogen transfer and electron-donating groups slowing it down (entries 1 and 2).[18] Interestingly, ketimines were not converted at all (entry 3), suggesting either a critical role of the α proton of the imine or steric constraints that hamper or even prevent substrate binding. In contrast to analogous carbonyl substrates, aliphatic and benzylic aldimines are poor substrates and need longer reaction times to reach substantial conversion (entries 4−6).

Base-Free Transfer Hydrogenation. Because of the potentially zwitterionic resonance structure and hence ambiguous donor properties of the PYA ligand in these iridium complexes **4a**−**4e**, we investigated transfer hydrogenation of more challenging substrates such as aldehydes.[18] The iridium complex **4d** was used as the catalyst precursor for the reduction of benzaldehyde under base-assisted standard conditions (refluxing *i*PrOH, 1 mol % catalyst loading, and 10 mol % KOH; Scheme 2). Essentially, full conversion of the substrate was achieved within less than 5 min [turnover frequency (TOF) > 1200 h^{-1}]; however, the yield of benzyl alcohol was only 50%. Isolation of the products revealed benzoic acid and benzoate as the second products, as expected from the Cannizzaro reaction.[26] However, no esters were formed under these reaction conditions.[27] Identical results were obtained when the catalyst loading was lowered to 0.01 mol %, but in this case, longer reaction times of up to 30 min were needed to reach maximum conversion. To establish the role of complex **4d** in this reaction, blank reactions in the presence of base but in the absence of complex **4d** were carried out, and they indeed showed the formation of benzyl alcohol and benzoic acid, although at a significantly slower rate. The metal-free reaction reached 25% conversion after 5 min and 65% after 30 min. In contrast, the **4d**-catalyzed reaction was complete within 5 min (at 1 mol % loading) and at 30 min at 0.01 mol % **4d**, suggesting a catalytic effect of the iridium complex. Moreover, the alcohol/acid product ratio was always 1:2, as opposed to the 1:1 ratio observed in runs in the presence of **4d**. When catalytic runs with **4d** were performed under an anaerobic argon atmosphere, the ratio of products was unaffected and remained at a 1:1 mixture of alcohol and acid. The rates and product ratio indicate that complex **4d** is accelerating the Cannizzaro reaction by about an order of magnitude and that the complex itself favors the reductive process and formation of the benzyl alcohol. These observations prompted us to investigate the hydrogen transfer activity of complex **4d** under base-free reaction conditions.

When the metal-catalyzed reaction with benzaldehyde was performed in neat *i*PrOH and without the addition of any base, aldehyde conversion was much slower, yet it reached 85% within 24 h. In contrast to the base-mediated reaction, the base-free procedure was completely selective and afforded exclusively benzyl alcohol as the product of transfer hydrogenation. Base-free transfer hydrogenation has been suggested

DOI: 10.1021/acs.inorgchem.7b01654
Inorg. Chem. XXXX, XXX, XXX−XXX

Table 5. Catalytic Transfer Hydrogenation of Different Imines[a]

entry	substrate	product	4 h yield (%)	24 h yield (%)[b]
1	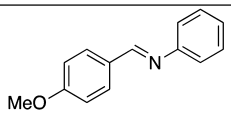	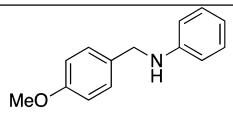	55	79
2	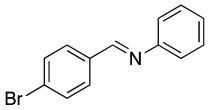	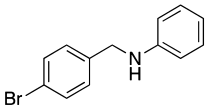	99[c]	n.d.
3	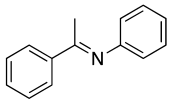	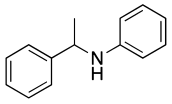	<5	<5
4	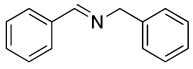	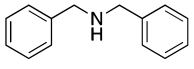	5	47
5	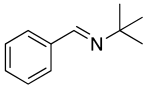	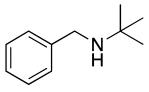	21	62
6	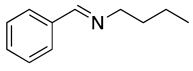	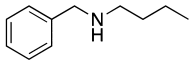	21	90

[a]General conditions: imine (1.0 mmol), complex **4b** (0.01 mmol), KOH (50 μL, 2 M in H_2O, 0.1 mmol), hexamethylbenzene (0.16 mmol), *i*PrOH (5 mL), reflux temperature. [b]Determined by ^{1}H NMR spectroscopy (error ±3%) with hexamethylbenzene as the internal standard; n.d. = not determined. [c]After 3 h.

Scheme 2. Catalytic Transformation of Benzaldehyde in Different Conditions

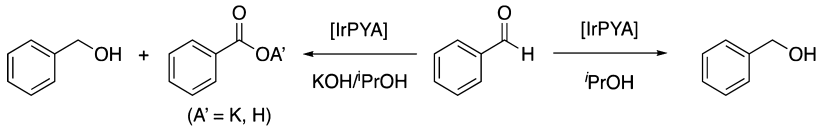

as an attractive methodology for the reduction of ketones and aldehydes because most alkali-metal bases traditionally used in transfer hydrogenation are corrosive and irreversibly alter the catalyst.[28] Stimulated by this activity, transfer hydrogenation of different substrates was tested under base-free conditions (Table 6). Substituted benzaldehydes are less active than the model substrate and did not give quantitative yields (entries 2 and 3). 4-Cyanobenzaldehyde is only moderately active, although we note that the nitrile group is not hydrogenated during the process and that the complex demonstrates excellent selectivity toward the carbonyl group (entry 4). In contrast to the ketone analogue in the base-assisted transfer hydrogenation, 2-pyridinecarboxaldehyde and aliphatic aldehydes are unsuitable substrates for transfer hydrogenation with no strong base added (entries 5 and 6). While aliphatic aldehydes may be too bulky to coordinate to the metal center under base-free conditions (entry 6), such conditions may favor pyridine coordination to the iridium center, which prevents conversion of heterocyclic substrates. In support of this model, conversion of benzaldehyde does not proceed in the presence of substoichiometric quantities of pyridine (<5% conversion after 2 h and 20% conversion after 24 h, compared to 59% and 85%, respectively, in the absence of pyridine). Hence, the presence of potentially coordinating functional groups in the substrate poisons the catalyst, which points to a distinctly different mechanism in comparison to the base-catalyzed reaction. In contrast, ketones such as acetophenone and benzophenone were essentially fully converted to the corresponding alcohol in 24 h. These considerably longer reaction times compared to the base-assisted transfer hydrogenation (3 h; cf. Table 3, entry 2) suggest a different mechanistic pathway for the base-free reaction compared to the KOH-mediated hydrogen transfer. We suggest that the base-catalyzed transfer hydrogenation conditions rapidly lead to the formation of the Ir−H species (i.e., the chlorides in complexes **4a**−**4e** are rapidly exchanged for hydrides), and hydrogenation then follows through insertion of the carbonyl group into the Ir−H bond. In contrast, under base-free conditions, *i*PrOH coordination to the metal center must occur to provide the—potentially ligand-assisted—dehydrogenation, and this coordination is unfavorable in the presence of stronger coordinating substrates such as the pyridyl unit in pyridylcarboxylate. The high conversions of benzaldehyde derivatives with complexes **4a**−**4e** suggest promising opportunities for base-free catalytic reactions using PYA ligands.

Catalytic Hydrosilylation of Phenylacetylene. Similar to transfer hydrogenation, hydrosilylation typically requires the transient formation of a metal hydride intermediate.[29] Prompted by the support established for a monohydride mechanism in transfer hydrogenation, we were therefore interested in evaluating the PYA complexes as catalyst precursors for the hydrosilylation of terminal alkynes. Three isomeric vinylsilane derivatives are usually obtained in this reaction, namely, $\beta(Z)$- and $\beta(E)$-vinylsilane as the products

DOI: 10.1021/acs.inorgchem.7b01654
Inorg. Chem. XXXX, XXX, XXX−XXX

Table 6. Base-Free Transfer Hydrogenation of Aldehydes and Ketones[a]

entry	substrate	product	yield at 2 h (%)	yield at 24 h (%)
1	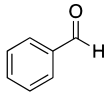	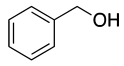	59	85
2	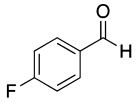	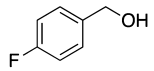	49	71
3	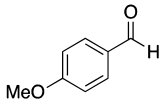	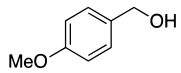	16	24
4	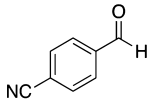	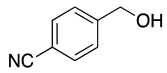	23	39
5	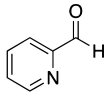	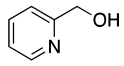	<5	<5
6	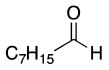	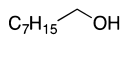	<5	<5
7	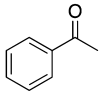	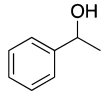	35	99
8	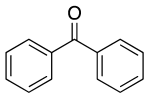	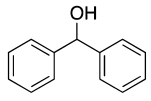	14	86

[a]General conditions: aldehyde or ketone (1.0 mmol), complex **4e** (0.01 mmol), hexamethylbenzene (0.16 mmol), *i*PrOH (5 mL), reflux temperature. [b]Determined by ^{1}H NMR spectroscopy (error ±3%) with hexamethylbenzene as the internal standard.

Table 7. Hydrosilylation of Phenylacetylene with PYA Iridium(III) Complexes[a]

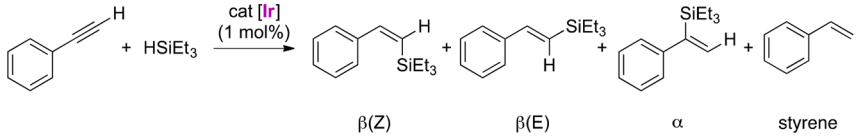

					selectivity			
entry	complex	*T* (°C)	time (h)	conv (%)	*β*(*Z*)	*β*(*E*)	*α*	styrene
1	**4a**	26	2	78	90	4	3	3
2	**4b**	26	2	89	95	2	2	1
3	**4c**	26	2	75	92	2	2	4
4	**4d**	26	2	94	95	1	3	1
5	**4e**	26	2	68	95	1	3	1
6	$[IrCp^*Cl_2]_2$	26	0.5/2	95/99	92/91	3/4	3/3	2/2
7	**4a**	40	1	99	93	3	2	2
8	**4b**	40	0.25	99	93	2	3	2
9	**4c**	40	0.33	99	94	2	3	1
10	**4d**	40	0.33	99	95	1	3	1
11	**4e**	40	0.5	99	95	1	3	1
12	$[IrCp^*Cl_2]_2$	40	0.25/2	99/99	95/91	1/4	3/3	1/2

[a]General conditions: phenylacetylene (0.18 mmol), triethylsilane (0.19 mmol), hexamethylbenzene (0.02 mmol), and catalyst (0.0018 mmol, 1 mol %) in either CH_2Cl_2 (26 °C) or $CHCl_3$ (40 °C). Conversion and selectivities were measured by ^{1}H NMR spectroscopy (error ±3%) with hexamethylbenzene as the internal standard.

from anti-Markovnikov addition and 2-silyl-1-alkene (*α* isomer) from Markovnikov addition (Table 7). In addition, the formation of the dehydrogenative silylation product, i.e., the corresponding silylacetylene as well as the unsubstituted alkene

DOI: 10.1021/acs.inorgchem.7b01654
Inorg. Chem. XXXX, XXX, XXX−XXX

due to desilylation, has also been observed in this reaction, in particular when sterically demanding alkynes or silanes were used.[29b] Hence, control of the regio- and stereoselectivity of this reaction remains a key issue. Numerous hydrosilylation studies have been performed using platinum group metal catalysts, in particular, with platinum,[30] ruthenium(II),[31] iridium(I), or rhodium(I).[32] However, only a few examples were reported starting from an iridium(III) complex as the catalyst precursor.[33]

Hence, complexes **4a**−**4e** were investigated as catalyst precursors for the hydrosilylation of phenylacetylene in the presence of a small excess of Et_3SiH as the silylating agent. A high catalytic efficiency was observed when the reaction was performed in CD_2Cl_2 at room temperature using a 1 mol % catalyst loading, reaching essentially quantitative conversion in 2 h (Table 7). The reaction proceeds with excellent selectivity (>90%) toward the $\beta(Z)$ isomer with only trace amounts of styrene, $\beta(E)$, and α isomers (entries 1−5).[34] Because formation of the $\beta(E)$ isomer is typically a postcatalytic process,[35] we assume that isomerization is suppressed by the presence of the PYA ligand, which prevents coordination of the $\beta(Z)$ isomer to the iridium center as a first step en route to formation of the Z isomer.

Similar to transfer hydrogenation, the methoxy substitution pattern requires optimization rather than maximization to reach the highest catalytic activity. The best performance was observed with catalyst precursors **4b** and **4d** containing one and two methoxy substituents, respectively, although the differences are not very pronounced. Complexes **4a** and **4e** are the least active, presumably for reasons similar to those discussed for transfer hydrogenation (see above); i.e., **4a** lacks the activating methoxy substituents, while for **4e**, substrate coordination and activation may be hindered for steric reasons. In contrast to previous studies using $[IrCp^*Cl_2]_2$ as the catalyst precursor,[35] no isomerization toward the $\beta(E)$ isomer was detected, presumably because of the constrained space around the catalytically active metal center imposed by the rigid chelation of the C,N-bidentate PYA ligand. This model is in agreement with the reactivity pattern observed in transfer hydrogenation, viz., moderate conversion of pyridyl ketones and poor conversion of sterically demanding (e.g., open-chain aliphatic) substrates. Moreover, this selectivity underpins the relevance of the PYA ligand because simple $[IrCp^*Cl_2]_2$ catalyzes the hydrosilylation faster but leads to a gradual increase in isomerization after completion of the reaction (entries 6 and 12), consistent with previous reports.[35] When the reaction temperature for hydrosilylation was raised to 40 °C, both the activity and selectivity toward the $\beta(Z)$ isomer increased (entries 7−11). When using complex **4b**, full conversion and 93% selectivity were noted after 15 min of reaction (entry 8). Complex **4d** required only slightly longer to reach the same conversion (20 min) and produced the $\beta(Z)$ isomer in 95% selectivity (entry 10). These preliminary investigations therefore suggest a high potential for these PYA iridium complexes for the selective transformation of acetylenes. While less pronounced than in transfer hydrogenation, tailoring of the aryl unit of the PYA ligand in complexes **4a**−**4e** provides an efficient methodology to optimize the catalyst activity.

CONCLUSIONS

A new family of Ir(C^N)Cp*-type complexes containing methoxy-substituted PYA ligands has been successfully prepared. The incorporation of one, two, or three methoxy groups in the phenyl ring was achieved without affecting the ease of ligand preparation or subsequent cyclometalation with iridium(III). Spectroscopic and crystallographic analyses indicate no structural distortion imparted by the methoxy groups, and therefore this methodology allows for the electronic parameters at the metal center to be tailored selectively. Such tailoring was demonstrated in transfer hydrogenation and hydrosilylation catalysis, which revealed a delicate balance and a nonlinear correlation between the number of donor groups and the catalytic activity. These results emphasize the importance of synthetic strategies for subtle ligand modifications in order to optimize the catalytic performance. The scanning of different substrates in transfer hydrogenation and hydrosilylation suggests that the bidentate PYA ligand remains coordinated to the Ir(Cp*) fragment and imparts a sterically constrained catalytic center, which has direct consequences on the catalyst activity and selectivity. Specifically, steric constraints prevent the coordination and conversion of bulky substrates, disfavor isomerization processes, and hence increase the selectivity in hydrosilylation, and finally they put limitations on the substituent incorporation to the phenyl unit of the PYA ligand. In addition, this work demonstrates that PYA ligands, still largely underexplored, offer vast synthetic opportunities for modifications, and together with their flexible donor structure, they constitute an attractive class of ligands for transition-metal catalysis. In particular, we have developed a protocol for base-free transfer hydrogenation of aldehydes, which under classic conditions with a base rapidly disproportionate to give large amounts of carboxylic acids instead.

EXPERIMENTAL PART

General Information. The metal precursor salt $[IrCp^*Cl_2]_2$,[36] compounds **1a**, **2a**, and **3a** and iridium complexes **4a**, **5a**, and **6a** were all synthesized as reported in the literature.[10b] All other reagents were commercially available and were used as received. Unless specified otherwise, NMR spectra were recorded at 25 °C on Bruker spectrometers operating at 300 or 400 MHz (^{1}H NMR) and 100 MHz (^{13}C NMR). Chemical shifts (δ in ppm and coupling constants J in Hz) were referenced to residual solvent signals (^{1}H and ^{13}C). Assignments are based on homo- and heteronuclear shift correlation spectroscopy. The purity of the bulk samples of the complexes has been established by NMR spectroscopy and by elemental analysis, which were performed at the Microanalytic Laboratory, University of Bern, using a Thermo Scientific Flash 2000 CHNS-O elemental analyzer. The residual solvent was confirmed by NMR spectroscopy and also by X-ray structure determinations. HR-MS was carried out with a Thermo Scientific LTQ Orbitrap XL (ESI-TOF) spectrometer.

General Procedure for the Formation of Amides 1b−1e. A solution of acyl chloride (11 mmol) in tetrahydrofuran (THF; 10 mL) was added dropwise at 0 °C into a solution of 4-aminopyridine (1.19 mL, 10 mmol) and NEt_3 (1.50 mL, 11 mmol) in THF (30 mL), which resulted in the formation of an immediate white precipitate. The reaction was slowly warmed to room temperature and stirred for 3 h. The formed precipitate was removed by filtration and washed with THF (50 mL). All filtrates were collected and the volatiles removed in vacuo to give a white solid, which was purified via column chromatography (SiO_2; 95:5 CH_2Cl_2/MeOH). All solvents were removed to yield the product as white solids.

Compound ***1b***. This compound was prepared according to the general procedure from 2-methoxybenzoyl chloride (1.877 g, 11 mmol). Yield: 1.750 g, 77%. ^{1}H NMR (300 MHz, DMSO-d_6): δ 10.55 (s, 1H, NH), 8.48 (d, $^3J_{HH}$ = 6.5 Hz, 2H, CH_{pyr}), 7.78 (d, $^3J_{HH}$ = 6.5 Hz, 2H, CH_{pyr}), 7.58−7.44 (m, 3H, CH_{Ph}), 7.23−7.17 (m, 1H, CH_{Ph}), 3.84 (s, 3H, OCH_3). ^{13}C{^{1}H} NMR (100 MHz, DMSO-d_6): δ 166.2 (CO), 159.2 (C_{Ph}), 150.3 (CH_{pyr}), 145.8 (C_{pyr}), 135.6 (C_{Ph}), 129.7

DOI: 10.1021/acs.inorgchem.7b01654
Inorg. Chem. XXXX, XXX, XXX−XXX

(CH_{Ph}), 120.0 (CH_{Ph}), 117.8 (CH_{Ph}), 114.0 (CH_{pyr}), 113.1 (CH_{Ph}), 55.4 (OCH_3). HR-MS. Calcd for $C_{13}H_{13}N_2O_2$ ($[M + H]^+$): m/z 229.0977. Calcd: m/z 229.0960. Elem. anal. Calcd for $C_{13}H_{13}N_2O_2$: C, 68.41; H, 5.30; N, 12.27. Found: C, 67.64; H, 5.00; N, 12.32.

Compound ***1c***. This compound was prepared according to the general procedure from 4-methoxybenzoyl chloride (1.877 g, 11 mmol). Yield: 1.990 g, 87%. ^{1}H NMR (300 MHz, DMSO-d_6): δ 10.42 (s, 1H, NH), 8.46 (d, $^3J_{HH}$ = 6.4 Hz, 2H, CH_{pyr}), 7.97 (d, $^3J_{HH}$ = 8.8 Hz, 2H, CH_{Ph}), 7.78 (d, $^3J_{HH}$ = 6.4 Hz, 2H, CH_{pyr}), 7.09 (d, $^3J_{HH}$ = 8.9 Hz, 2H, CH_{Ph}), 3.85 (s, 3H, OCH_3). $^{13}C\{^1H\}$ NMR (100 MHz, DMSO-d_6): δ 165.7 (CO), 162.3 (C_{Ph}), 150.2 (CH_{pyr}), 146.1 (C_{pyr}), 129.9 (CH_{Ph}), 126.2 (C_{Ph}), 113.9 (CH_{pyr}), 113.7 (CH_{Ph}), 55.5 (OCH_3). HR-MS. Calcd for $C_{13}H_{14}N_2O_2$ ($[M + H]^+$): m/z 229.0977. Calcd m/z 229.0962. Elem. anal. Calcd for $C_{13}H_{13}N_2O_2$: C, 68.41; H, 5.30; N, 12.27. Found: C, 68.21; H, 4.89; N, 12.20.

Compound ***1d***. This compound was prepared according to the general procedure from 3,5-dimethoxybenzoyl chloride (2.206 g, 11 mmol). Yield: 2.207 g, 85%. ^{1}H NMR (300 MHz, DMSO-d_6): δ 10.50 (s, 1H, NH), 8.48 (d, $^3J_{HH}$ = 6.4 Hz, 2H, CH_{pyr}), 7.77 (d, $^3J_{HH}$ = 6.4 Hz, 2H, CH_{pyr}), 7.10 (d, $^4J_{HH}$ = 2.4 Hz, 2H, CH_{Ph}), 6.76 (t, $^4J_{HH}$ = 2.3 Hz, 1H, CH_{Ph}), 3.83 (s, 6H, OCH_3). $^{13}C\{^1H\}$ NMR (100 MHz, DMSO-d_6): δ 166.0 (CO), 160.4 (C_{Ph}), 150.3 (CH_{pyr}), 145.8 (C_{pyr}), 136.2 (C_{Ph}), 114.7 (CH_{pyr}), 105.8 (CH_{Ph}), 103.7 (CH_{Ph}), 55.6 (OCH_3). HR-MS. Calcd for $C_{14}H_{15}N_2O_3$ ($[M + H]^+$): m/z 259.1083. Calcd: m/z 259.1071. Elem. anal. Calcd for $C_{14}H_{14}N_2O_3$: C, 65.11; H, 5.46; N, 10.85. Found: C, 65.01; H, 5.10; N, 10.75.

Compound ***1e***. This compound was prepared according to the general procedure from 3,4,5-dimethoxybenzoyl chloride (2.537 g, 11 mmol). Yield: 2.134 g, 74%. ^{1}H NMR (300 MHz, DMSO-d_6): δ 10.45 (s, 1H, NH), 8.50 (d, $^3J_{HH}$ = 6.4 Hz, 2H, CH_{pyr}), 7.76 (d, $^3J_{HH}$ = 6.4 Hz, 2H, CH_{pyr}), 7.29 (s, 2H, CH_{Ph}), 3.89 (s, 6H, OCH_3), 3.75 (s, 3H, OCH_3). $^{13}C\{^1H\}$ NMR (100 MHz, DMSO-d_6): δ 165.8 (CO), 152.7 (s, C_{Ph}), 150.3 (CH_{pyr}), 145.9 (C_{pyr}), 140.8 (C_{Ph}), 129.3 (C_{Ph}), 114.1 (CH_{pyr}), 105.6 (CH_{Ph}), 60.1 (OCH_3), 56.2 (OCH_3). HR-MS. Calcd for $C_{14}H_{17}N_2O_4$ ($[M + H]^+$): m/z 289.1188. Calcd: m/z 289.1176. Elem. anal. Calcd for $C_{15}H_{16}N_2O_4 \cdot 0.25H_2O$: C, 61.53; H, 5.68; N, 9.57. Found: C, 61.51; H, 5.37; N, 9.24.

General Procedure for the Formation of Pyridinium Salts 2. Compound **1** (2.0 mmol) was dissolved in MeCN (15 mL) in a pressure tube. MeI (187 μL, 3.0 mmol) was added, and the reaction was stirred for 18 h at 80 °C. The solution was cooled to room temperature and concentrated to 5 mL. Et_2O (50 mL) was added, affording compound **2** as a yellow solid, which was collected by filtration.

Compound ***2b***. Compound **2b** was prepared according to the general procedure from **1b**. Yield: 715 mg, 97%. ^{1}H NMR (300 MHz, DMSO-d_6): δ 11.43 (s, 1H, NH), 8.78 (d, $^3J_{HH}$ = 7.3 Hz, 2H, CH_{pyr}), 8.21 (d, $^3J_{HH}$ = 7.3 Hz, 2H, CH_{pyr}), 7.68–7.55 (m, 2H, CH_{Ph}), 7.26 (d, $^3J_{HH}$ = 8.3 Hz, 1H, CH_{Ph}), 7.13 (t, $^3J_{HH}$ = 7.6 Hz, 1H, CH_{Ph}), 4.21 (s, 3H, NCH_3), 3.91 (s, 3H, OCH_3). $^{13}C\{^1H\}$ NMR (100 MHz, DMSO-d_6): δ 166.8 (CO), 156.7 (C_{Ph}), 151.2 (C_{pyr}), 146.3 (CH_{pyr}), 133.5 (CH_{Ph}), 129.8 (CH_{Ph}), 123.3 (C_{Ph}), 120.6 (CH_{Ph}), 115.0 (CH_{pyr}), 112.3 (CH_{Ph}), 56.1 (OCH_3), 46.4 (NCH_3). HR-MS. Calcd for $C_{14}H_{15}N_2O_2$ ($[M - I]^+$): m/z 243.1128. Found: m/z 243.1124. Elem. anal. Calcd for $C_{14}H_{15}N_2O_2I$: C, 45.42; H, 4.08; N, 7.57. Found: C, 45.15; H, 3.75; N, 7.66.

Compound ***2c***. Compound **2c** was prepared according to the general procedure from **1c** (456 mg, 2.0 mmol). Yield: 646 mg, 87%. ^{1}H NMR (300 MHz, DMSO-d_6): δ 11.33 (s, 1H, NH), 8.76 (d, $^3J_{HH}$ = 7.2 Hz, 2H, CH_{pyr}), 8.26 (d, $^3J_{HH}$ = 7.2 Hz, 2H, CH_{pyr}), 8.03 (d, $^3J_{HH}$ = 8.8 Hz, 2H, CH_{Ph}), 7.14 (d, $^3J_{HH}$ = 8.8 Hz, 2H, CH_{Ph}), 4.19 (s, 3H, NCH_3), 3.87 (s, 6H, OCH_3). $^{13}C\{^1H\}$ NMR (100 MHz, DMSO-d_6): δ 166.3 (CO), 163.2 (C_{Ph}), 152.1 (C_{pyr}), 145.7 (CH_{pyr}), 130.5 (CH_{Ph}), 124.7 (C_{Ph}), 115.5 (CH_{pyr}), 114.0 (CH_{Ph}), 56.0 (OCH_3), 46.4 (NCH_3). HR-MS. Calcd for $C_{14}H_{15}N_2O_2$ ($[M - I]^+$): m/z 243.1128. Found; m/z 243.1117. Elem. anal. Calcd for $C_{14}H_{15}N_2O_2I$: C, 45.42; H, 4.08; N, 7.57. Found: C, 45.10; H, 3.78; N, 7.68.

Compound ***2d***. Compound **2d** was prepared according to the general procedure from **1d** (517 mg, 2.0 mmol). Yield: 735 mg, 92%. ^{1}H NMR (300 MHz, DMSO-d_6): δ 11.43 (s, 1H, NH), 8.79 (d, $^3J_{HH}$ = 7.0 Hz, 2H, CH_{pyr}), 8.27 (d, $^3J_{HH}$ = 7.0 Hz, 2H, CH_{pyr}), 7.16 (d, $^4J_{HH}$ = 2.2 Hz, 2H, CH_{Ph}), 6.85 (t, $^4J_{HH}$ = 2.2 Hz, 1H, CH_{Ph}), 4.21 (s, 3H, NCH_3), 3.86 (s, 6H, OCH_3). $^{13}C\{^1H\}$ NMR (100 MHz, DMSO-d_6): δ 166.8 (CO), 160.6 (C_{Ph}), 151.8 (C_{pyr}), 145.9 (CH_{pyr}), 138.9 (C_{Ph}), 115.5 (CH_{pyr}), 106.3 (CH_{Ph}), 104.5 (CH_{Ph}), 55.7 (OCH_3), 46.4 (NCH_3). HR-MS. Calcd for $C_{15}H_{17}N_2O_3$ ($[M - I]^+$): m/z 273.1234. Found; m/z 273.1228. Elem. anal. Calcd for $C_{15}H_{17}N_2O_3I$: C, 45.02; H, 4.28; N, 7.00. Found: C, 44.80; H, 4.08; N, 7.13.

Compound ***2e***. Compound **2e** was prepared according to the general procedure from **1e** (577 mg, 2.0 mmol). Yield: 792 mg, 92%. ^{1}H NMR (300 MHz, DMSO-d_6): δ 11.36 (s, 1H, NH), 8.80 (d, $^3J_{HH}$ = 7.0 Hz, 2H, CH_{pyr}), 8.26 (d, $^3J_{HH}$ = 7.0 Hz, 2H, CH_{pyr}), 7.34 (s, 2H, CH_{Ph}), 4.22 (s, 3H, NCH_3), 3.90 (s, 6H, OCH_3), 3.78 (s, 3H, OCH_3). $^{13}C\{^1H\}$ NMR (100 MHz, DMSO-d_6): δ 166.6 (CO), 152.8 (C_{Ph}), 151.9 (C_{pyr}), 145.9 (CH_{pyr}), 141.7 (C_{Ph}), 127.9 (C_{Ph}), 115.5 (CH_{pyr}), 106.2 (CH_{Ph}), 60.2 (OCH_3), 56.3 (OCH_3), 46.4 (NCH_3). HR-MS. Calcd for $C_{16}H_{19}N_2O_4$ ($[M - I]^+$): m/z 303.1339. Found: m/z 303.1328. Elem. anal. Calcd for $C_{16}H_{19}N_2O_4I$: C, 44.67; H, 4.45; N, 6.51. Found: C, 44.58; H, 4.12; N, 6.66.

General Procedure for Synthesis of the Pyridylidene Amides 3b–3e. A suspension of the pyridinium salt **2** (1.0 mmol) in CH_2Cl_2 (10 mL) was placed in a separating funnel. Aqueous NaOH (15 mL, 2M) was added. After vigorous mixing, the organic phase was collected. The aqueous layer was extracted with CH_2Cl_2 (3 × 15 mL), and the combined organic layers were dried over anhydrous Na_2SO_4 and filtered. All volatiles were removed, thus giving free ligand **3** as white-yellow solids, which were purified by recrystallization from pentane.

Compound ***3b***. Compound **3b** was synthesized following the general procedure from compound **2b** (370 mg, 1.0 mmol). Yield: 160 mg, 66%. ^{1}H NMR (300 MHz, DMSO-d_6): δ 7.91 (d, $^3J_{HH}$ = 7.5 Hz, 2H, CH_{pyr}), 7.38 (dd, $^3J_{HH}$ = 7.5 Hz, $^4J_{HH}$ = 1.8 Hz, 1H, CH_{Ph}), 7.31 (d, $^3J_{HH}$ = 7.5 Hz, 2H, CH_{pyr}), 7.28–7.23 (m, 1H, CH_{Ph}), 6.97 (d, $^3J_{HH}$ = 8.0 Hz, 1H, CH_{Ph}), 6.88 (t, $^3J_{HH}$ = 7.4 Hz, 1H, CH_{Ph}), 3.80 (s, 3H, NCH_3), 3.72 (s, 3H, OCH_3). $^{13}C\{^1H\}$ NMR (100 MHz, DMSO-d_6): δ 176.3 (CO), 163.0 (C_{pyr}), 156.4 (C_{Ph}), 141.7 (CH_{pyr}), 132.5 (C_{Ph}), 129.0 (CH_{Ph}), 128.7 (CH_{Ph}), 119.6 (CH_{Ph}), 117.1 (CH_{pyr}), 111.9 (CH_{Ph}), 56.1 (OCH_3), 46.4 (NCH_3). HR-MS. Calcd for $C_{14}H_{15}N_2O_2$ ($[M + H]^+$): m/z 243.1134. Found: m/z 243.1122. Elem. anal. Calcd for $C_{14}H_{14}N_2O_2$: C, 69.41; H, 5.82; N, 11.56. Found: C, 69.65; H, 5.42; N, 11.22.

Compound ***3c***. Compound **3c** was synthesized following the general procedure from compound **2c** (370 mg, 1.0 mmol). Yield: 155 mg, 64%. ^{1}H NMR (300 MHz, DMSO-d_6): δ 8.07 (d, $^3J_{HH}$ = 8.8 Hz, 2H, CH_{Ph}), 7.90 (d, $^3J_{HH}$ = 7.4 Hz, 2H, CH_{pyr}), 7.40 (d, $^3J_{HH}$ = 7.4 Hz, 2H, CH_{pyr}), 6.91 (d, $^3J_{HH}$ = 8.8 Hz, 2H, CH_{pyr}), 3.80 (s, 3H, NCH_3), 3.79 (s, 3H, OCH_3). $^{13}C\{^1H\}$ NMR (100 MHz, DMSO-d_6): δ 173.8 (CO), 163.8 (C_{Ph}), 161.0 (C_{pyr}), 141.6 (CH_{pyr}), 132.4 (C_{Ph}), 130.6 (CH_{Ph}), 117.4 (CH_{pyr}), 112.8 (CH_{Ph}), 55.2 (OCH_3), 43.7 (NCH_3). HR-MS. Calcd for $C_{14}H_{15}N_2O_2$ ($[M + H]^+$): m/z 243.1134. Found: m/z 243.1121. Elem. anal. Calcd for $C_{14}H_{14}N_2O_2$: C, 69.41; H, 5.82; N, 11.56. Found: C, 68.66; H, 5.27; N, 12.00.

Compound ***3d***. Compound **3d** was synthesized following the general procedure from compound **2d** (400 mg, 1.0 mmol). Yield: 233 mg, 86%. ^{1}H NMR (300 MHz, DMSO-d_6): δ 7.98 (d, $^3J_{HH}$ = 7.5 Hz, 2H, CH_{pyr}), 7.47 (d, $^3J_{HH}$ = 7.5 Hz, 2H, CH_{pyr}), 7.31 (d, $^4J_{HH}$ = 2.4 Hz, 2H, CH_{Ph}), 6.56 (t, $^4J_{HH}$ = 2.4 Hz, 1H, CH_{Ph}), 3.84 (s, 3H, NCH_3), 3.77 (s, 6H, OCH_3). $^{13}C\{^1H\}$ NMR (100 MHz, DMSO-d_6): δ 173.2 (CO), 164.0 (C_{pyr}), 159.8 (C_{Ph}), 142.3 (CH_{pyr}), 141.9 (C_{Ph}), 117.8 (CH_{pyr}), 106.4 (CH_{Ph}), 102.4 (CH_{Ph}), 55.1 (OCH_3), 43.8 (NCH_3). HR-MS. Calcd for $C_{15}H_{17}N_2O_3$ ($[M + H]^+$): m/z 273.1239. Found: m/z 273.1220. Elem. anal. Calcd for $C_{15}H_{16}N_2O_3$: C, 66.16; H, 5.92; N, 10.29. Found: C, 65.75; H, 5.50; N, 10.75.

Compound ***3e***. Compound **3e** was synthesized following the general procedure from compound **2e** (430 mg, 1.0 mmol). Yield: 252 mg, 84%. ^{1}H NMR (300 MHz, DMSO-d_6): δ 7.96 (d, $^3J_{HH}$ = 7.1 Hz, 2H, CH_{pyr}), 7.48 (s, 2H, CH_{Ph}), 7.45 (d, $^3J_{HH}$ = 7.5 Hz, 2H, CH_{pyr}), 3.83 (s, 3H, NCH_3), 3.82 (s, 6H, OCH_3), 3.71 (s, 3H, OCH_3). $^{13}C\{^1H\}$ NMR (100 MHz, DMSO-d_6): δ 173.2 (CO), 164.0 (C_{pyr}), 152.0 (C_{Ph}), 141.8 (CH_{pyr}), 139.5 (C_{Ph}), 135.4 (C_{Ph}), 117.7 (CH_{pyr}),

DOI: 10.1021/acs.inorgchem.7b01654
Inorg. Chem. XXXX, XXX, XXX–XXX

106.0 (CH_{Ph}), 60.0 (OCH_3), 55.7 (OCH_3), 43.8 (NCH_3). HR-MS. Calcd for $C_{16}H_{19}N_2O_4$ ($[M + H]^+$): m/z 303.1345. Found: m/z 303.1327. Elem. anal. Calcd for $C_{16}H_{18}N_2O_4$: C, 63.56; H, 6.00; N, 9.27. Found: C, 63.90; H, 5.87; N, 10.89.

General Procedure for the Synthesis of Complexes 4b−4e. Compound **3** (0.4 mmol), $[IrCp^*Cl_2]_2$ (120 mg, 0.15 mmol), and NaOAc (33 mg, 0.4 mmol) were dissolved in CH_2Cl_2 and stirred at room temperature for 18 h. All volatiles were removed under reduced pressure, and the crude solid was purified by column chromatography (SiO_2; 98:2 CH_2Cl_2/MeOH), thus yielding **4** as orange solids.

Compound 4b. Compound **4b** was prepared according to the general procedure from **3b** (97 mg, 0.40 mmol). Yield: 139 mg, 77%. ^1H NMR (400 MHz, $CDCl_3$): δ 8.27 (d, $^3J_{HH}$ = 7.1 Hz, 2H, CH_{pyr}), 7.47 (d, $^3J_{HH}$ = 7.4 Hz, 2H, CH_{pyr}), 7.31 (d, $^3J_{HH}$ = 7.3 Hz, 1H, CH_{Ph}), 7.14 (t, $^3J_{HH}$ = 7.8 Hz, 1H, CH_{Ph}), 6.49 (d, $^3J_{HH}$ = 7.8 Hz, 1H, CH_{Ph}), 3.89 (s, 3H, OCH_3), 3.53 (s, 3H, NCH_3), 1.47 (s, 15H, Cp^*CH_3). $^{13}C\{^1H\}$ NMR (100 MHz, $CDCl_3$): δ 182.3 (CO), 163.2 (C_{Ph}), 161.6 (C_{pyr}), 160.3 (C_{Ph}), 140.6 (CH_{pyr}), 132.7 (CH_{Ph}), 129.4 (CH_{Ph}), 127.5 (C_{Ph}), 120.6 (CH_{pyr}), 105.1 (CH_{Ph}), 87.5 (C_{Cp^*}), 55.3 (OCH_3), 44.8 (NCH_3), 9.2 (CH_3Cp^*). HR-MS. Calcd for $C_{24}H_{29}IrN_2O_2$ ($[M - Cl]^+$): m/z 605.1541. Found: 605.1522. Elem anal. Calcd for $C_{24}H_{29}ClIrN_2O_2$: C, 47.71; H, 4.67; N, 4.64. Found: C, 47.67; H, 4.52; N, 4.61.

Compound 4c. This compound was prepared according to the general procedure from **3c** (97 mg, 0.40 mmol. Yield: 140 mg, 78%. ^1H NMR (400 MHz, $CDCl_3$): δ 8.29 (d, $^3J_{HH}$ = 7.0 Hz, 2H, CH_{pyr}), 7.58 (d, $^3J_{HH}$ = 8.4 Hz, 1H, CH_{Ph}), 7.51 (d, $^3J_{HH}$ = 7.3 Hz, 2H, CH_{pyr}), 7.27 (d, $^4J_{HH}$ = 2.5 Hz, 1H, CH_{Ph}), 6.53 (dd, $^3J_{HH}$ = 8.4 Hz, $^4J_{HH}$ = 2.5 Hz, 1H, CH_{Ph}), 3.88 (s, 3H, OCH_3), 3.47 (s, 3H, NCH_3), 1.47 (s, 15H, Cp^*CH_3). $^{13}C\{^1H\}$ NMR (100 MHz, $CDCl_3$): δ 182.7 (CO), 162.4 (C_{Ph}), 162.2 (C_{Ph}), 161.7 (C_{pyr}), 140.9 (CH_{pyr}), 134.4 (C_{Ph}), 129.6 (CH_{Ph}), 121.1 (CH_{pyr}), 119.8 (CH_{Ph}), 109.4 (CH_{Ph}), 87.3 (C_{Cp^*}), 55.2 (OCH_3), 45.3 (NCH_3), 9.2 (CH_3Cp^*). HR-MS. Calcd for $C_{24}H_{29}IrN_2O_2$ ($[M - Cl]^+$): m/z 605.1541. Found: m/z 605.1493. Elem anal. Calcd for $C_{24}H_{29}ClIrN_2O_2{\cdot}0.25CH_2Cl_2$: C, 46.50; H, 4.75; N, 4.47. Found: C, 46.31; H, 4.39; N, 4.47.

Compound 4d. The title compound was prepared according to the general procedure from **3d** (109 mg, 0.40 mmol). Yield: 162 mg, 75%. ^1H NMR (400 MHz, $CDCl_3$): δ 8.35 (d, $^3J_{HH}$ = 7.0 Hz, 2H, CH_{pyr}), 7.51 (d, $^3J_{HH}$ = 7.5 Hz, 2H, CH_{pyr}) 6.89 (d, $^4J_{HH}$ = 2.4 Hz, 1H, CH_{Ph}), 6.47 (d, $^4J_{HH}$ = 2.4 Hz, 1H, CH_{Ph}), 3.83 (s, 3H, OCH_3), 3.80 (s, 3H, OCH_3), 3.47 (s, 3H, NCH_3), 1.47 (s, 15H, Cp^*CH_3). $^{13}C\{^1H\}$ NMR (100 MHz, $CDCl_3$): δ 183.5 (CO), 163.1 (C_{Ph}), 161.7 (C_{pyr}), 157.4 (C_{Ph}), 142.0 (C_{Ph}), 141.0 (CH_{pyr}), 139.0 (C_{Ph}), 120.9 (CH_{pyr}), 103.6 (CH_{Ph}), 103.2 (CH_{Ph}), 87.3 (C_{Cp^*}), 56.0 (OCH_3), 55.6 (OCH_3), 45.6 (NCH_3), 9.2 (CH_3Cp^*). HR-MS. Calcd for $C_{25}H_{30}IrN_2O_3$ ($[M - Cl]^+$): m/z 599.1886. Found: m/z 599.1859. Elem anal. Calcd for $C_{25}H_{30}ClIrN_2O_3$: C, 47.35; H, 4.77; N, 4.42. Found: C, 47.92; H, 4.60; N, 4.38.

Compound 4e. Compound **4e** was prepared according to the general procedure from **3e** (121 mg, 0.40 mmol). Yield: 139 mg, 70%. ^1H NMR (400 MHz, $CDCl_3$): δ 8.39 (d, $^3J_{HH}$ = 7.0 Hz, 2H, CH_{pyr}), 7.52 (d, $^3J_{HH}$ = 7.3 Hz, 2H, CH_{pyr}) 7.14 (s, 1H, CH_{Ph}), 3.98 (s, 3H, OCH_3), 3.88 (s, 3H, OCH_3), 3.87 (s, 3H, OCH_3), 3.58 (s, 3H, NCH_3), 1.52 (s, 15H, Cp^*CH_3). $^{13}C\{^1H\}$ NMR (100 MHz, $CDCl_3$): δ 183.4 (CO), 161.5 (C_{pyr}), 156.4 (C_{Ph}), 150.1 (C_{Ph}), 146.8 (C_{Ph}), 140.6 (CH_{pyr}), 136.3 (C_{Ph}), 120.9 (CH_{pyr}), 108.3 (CH_{Ph}), 87.6 (C_{Cp^*}), 62.0 (OCH_3), 60.8 (OCH_3), 56.2 (OCH_3), 45.0 (NCH_3), 9.3 (CH_3Cp^*). HR-MS. Calcd for $C_{26}H_{32}IrN_2O_4$ ($[M - Cl]^+$): m/z 629.1991. Found: m/z 666.19744. Elem anal. Calcd for $C_{26}H_{32}ClIrN_2O_4$: C, 47.02; H, 4.86; N, 4.22. Found: C, 47.11; H, 4.59; N, 4.17.

General Procedure for Base-Assisted Catalytic Transfer Hydrogenation. A mixture of the catalyst precursor (0.01 mmol), anisole (110 μL, 1 mmol), or hexamethylbenzene (27 mg, 0.16 mmol) as the internal standard and KOH (2 M solution in H_2O, 50 μL, 0.1 mmol) in *i*PrOH (5 mL) was mixed in a one-neck round-bottomed flask in air (or argon if specified) and heated to reflux for 15 min. Then, substrate (1.0 mmol) was rapidly added, and aliquots (ca. 0.1 mL) were taken at set times and dissolved in CD_3OD, acetone-d^6, or $CDCl_3$. The reaction mixtures were analyzed by ^1H NMR spectroscopy. Conversions and yields were determined relative to anisole or hexamethylbenzene.

General Procedure for Base-Free Catalytic Transfer Hydrogenation. In a one-neck round-bottom flask open to air, a mixture of catalyst precursor (0.01 mmol), hexamethylbenzene (27 mg, 0.16 mmol) as internal standard and substrate (1.0 mmol) was refluxed in *i*PrOH (5 mL). Aliquots (ca. 0.1 mL) were taken at set times and dissolved in $CDCl_3$. The reaction mixtures were analyzed by ^1H NMR spectroscopy. Conversions and yields were determined relative to anisole or hexamethylbenzene.

General Procedure for Hydrosilylation of Phenylacetylene. Phenylacetylene (20 μL, 0.18 mmol), triethylsilane (30 μL, 0.19 mmol), and hexamethylbenzene (3.2 mg, 0.02 mmol) were dissolved in CD_2Cl_2 or $CDCl_3$ (0.5 mL) in an NMR tube under a normal atmosphere of air. The catalyst (1.8 μmol, 1 mol %) was added, and the reaction was followed by ^1H NMR spectroscopy at fixed times at either 26 or 40 °C.

Crystal Structure Determinations. Suitable crystals of **4b−4e** were mounted in air at ambient conditions and measured on an Oxford Diffraction SuperNova area-detector diffractometer at T = 173(2) K using mirror optics monochromated Mo Kα radiation (λ = 0.71073 Å) and filtered aluminum.[37] Data reduction was performed using the *CrysAlisPro* program.[38] The intensities were corrected for Lorentz and polarization effects, and an absorption correction based on the multiscan method using *SCALE3 ABSPACK* in *CrysAlisPro* was applied. The structures were solved by direct methods using *SHELXT*,[39] and all non-hydrogen atoms were refined anisotropically. All hydrogen atoms were placed in geometrically calculated positions and refined using a riding model, with each hydrogen atom assigned a fixed isotropic displacement parameter (1.2U_{eq} of its parent atom and 1.5U_{eq} for the methyl groups). Structures were refined on F^2 using full-matrix least-squares procedures. The weighting schemes were based on counting statistics and included a factor to downweight the intense reflections. All calculations were performed using the *SHELXL-2014* program.[39]

The asymmetric unit of compound **4b** contained two independent complex molecules and two molecules of the solvent. Careful checking did not reveal any obvious symmetry operation relating the two independent molecules. All investigated crystals of **4c** were systematically affected by an intergrowth nonmerohedral twinning. The data were therefore integrated and refined using reflections of both components, and each measured structure factor was fitted to the sum of all contributing components (HKLF5 option in *SHELX*). For the sample selected for structural analysis, compositions of $^1/_3$ and $^2/_3$ were refined (although other samples gave other ratios). All mounted crystals of **4d** were systematically affected by weak diffraction at high resolution, diffuse scattering, and spurious peaks at non-Bragg positions possibly, indicating the presence of many twin components. For this reason, the quality indices of the refinement are poorer and large residuals in the vicinity of the iridium atom are found, which could not be associated with a structural disorder. Further details are given in Tables S2−S5. Crystallographic data for all four structures have been deposited with the Cambridge Crystallographic Data Centre as supplementary publication numbers 1530958 (**4b**), 1530960 (**4c**), 1530961 (**4d**), and 1530959 (**4e**).

■ ASSOCIATED CONTENT

Supporting Information

The Supporting Information is available free of charge on the ACS Publications website at DOI: 10.1021/acs.inorgchem.7b01654.

Time−conversion profiles for catalytic experiments, crystallographic details, and NMR spectra of all compounds (PDF)

DOI: 10.1021/acs.inorgchem.7b01654
Inorg. Chem. XXXX, XXX, XXX−XXX

Accession Codes

CCDC 1530958−1530961 contain the supplementary crystallographic data for this paper. These data can be obtained free of charge via www.ccdc.cam.ac.uk/data_request/cif, or by emailing data_request@ccdc.cam.ac.uk, or by contacting The Cambridge Crystallographic Data Centre, 12 Union Road, Cambridge CB2 1EZ, UK; fax: +44 1223 336033.

AUTHOR INFORMATION

Corresponding Author

*E-mail: martin.albrecht@dcb.unibe.ch.

ORCID

Martin Albrecht: 0000-0001-7403-2329

Present Address

‡C.A.S.: Department of Chemistry, Queen's University, 90 Bader Lane, Kingston, Ontario, Canada.

Notes

The authors declare no competing financial interest.

ACKNOWLEDGMENTS

We acknowledge generous financial support from the European Research Council (Grant CoG 615653) and from the Swiss National Science Foundation (Grant 200021_162868 and R'equip Projects 206021_128724 and 206021_170755). C.A.S. thanks the Natural Science and Engineering Research Council of Canada, the Water Sumner Foundation, and Queen's University. We thank the group of Chemical Crystallography of the University of Bern for X-ray analysis of all reported structures.

REFERENCES

(1) Hartwig, J. *Organotransition Metal Chemistry*; University Science Books: Mill Valley, CA, 2010.

(2) (a) Khusnutdinova, J. R.; Milstein, D. Metal−Ligand Cooperation. *Angew. Chem., Int. Ed.* **2015**, *54*, 12236−12273. (b) Broere, D. L. J.; Plessius, R.; van der Vlugt, J. I. New avenues for ligand-mediated processes − expanding metal reactivity by the use of redox-active catechol, *o*-aminophenol and *o*-phenylenediamine ligands. *Chem. Soc. Rev.* **2015**, *44*, 6886−6915. (c) Grotjahn, D. B. Structures, Mechanisms, and Results in Bifunctional Catalysis and Related Species Involving Proton Transfer. *Top. Catal.* **2010**, *53*, 1009−1014.

(3) (a) Shvo, Y.; Czarkie, D.; Rahamim, Y.; Chodosh, D. F. A new group of ruthenium complexes: structure and catalysis. *J. Am. Chem. Soc.* **1986**, *108*, 7400−7402. (b) Ohkuma, T.; Ooka, H.; Hashiguchi, S.; Ikariya, T.; Noyori, R. Practical Enantioselective Hydrogenation of Aromatic Ketones. *J. Am. Chem. Soc.* **1995**, *117*, 2675−2676.

(4) (a) Gunanathan, C.; Ben-David, Y.; Milstein, D. Direct Synthesis of Amides from Alcohols and Amines with Liberation of H_2. *Science* **2007**, *317*, 790−792. (b) Kohl, S. W.; Weiner, L.; Schwartsburd, L.; Konstantinovski, L.; Shimon, L. J. W.; Ben-David, Y.; Iron, M. A.; Milstein, D. Consecutive Thermal H_2 and Light-Induced O_2 Evolution from Water Promoted by a Metal Complex. *Science* **2009**, *324*, 74−77. (c) Milstein, D. Discovery of Environmentally Benign Catalytic Reactions of Alcohols Catalyzed by Pyridine-Based Pincer Ru Complexes, Based on Metal−Ligand Cooperation. *Top. Catal.* **2010**, *53*, 915−923. (d) Gloaguen, Y.; Rebreyend, C.; Lutz, M.; Kumar, P.; Huber, M.; van der Vlugt, J. I.; Schneider, S.; de Bruin, B. An Isolated Nitridyl Radical-Bridged {Rh(N.)Rh} Complex. *Angew. Chem., Int. Ed.* **2014**, *53*, 6814−6818. (e) César, V.; Lugan, N.; Lavigne, G. A Stable Anionic N-Heterocyclic Carbene and Its Zwitterionic Complexes. *J. Am. Chem. Soc.* **2008**, *130*, 11286−11287. (f) Bruns, H.; Patil, M.; Carreras, J.; Vázquez, A.; Thiel, W.; Goddard, R.; Alcarazo, M. Synthesis and Coordination Properties of Nitrogen(I)-Based Ligands. *Angew. Chem., Int. Ed.* **2010**, *49*, 3680−3683.

(5) For selected classic NHC reviews, see: (a) Hahn, F. E.; Jahnke, M. C. Heterocyclic Carbenes: Synthesis and Coordination Chemistry. *Angew. Chem., Int. Ed.* **2008**, *47*, 3122−3172. (b) Arduengo, A. J.; Bertrand, G. Carbenes Introduction. *Chem. Rev.* **2009**, *109*, 3209−3210. (c) Melaimi, M.; Soleilhavoup, M.; Bertrand, G. Stable Cyclic Carbenes and Related Species beyond Diaminocarbenes. *Angew. Chem., Int. Ed.* **2010**, *49*, 8810−8849.

(6) For mesoionic NHCs, see: (a) Albrecht, M. Normal and Abnormal N-Heterocyclic Carbene Ligands: Similarities and Differences of Mesoionic C-Donor Complexes. *Adv. Organomet. Chem.* **2014**, *62*, 111−159. (b) Schuster, O.; Yang, L.; Raubenheimer, H. G.; Albrecht, M. Beyond Conventional *N*-Heterocyclic Carbenes: Abnormal, Remote, and Other Classes of NHC Ligands with Reduced Heteroatom Stabilization. *Chem. Rev.* **2009**, *109*, 3445−3478. (c) Donnelly, K. F.; Petronilho, A.; Albrecht, M. Application of 1,2,3-triazolylidenes as versatile NHC-type ligands: synthesis, properties, and application in catalysis and beyond. *Chem. Commun.* **2013**, *49*, 1145−1159.

(7) For low π-acidic properties of NHCs, see: (a) Back, O.; Henry-Ellinger, M.; Martin, C. D.; Martin, D.; Bertrand, G. ^{31}P NMR Chemical Shifts of Carbene−Phosphinidene Adducts as an Indicator of the π-Accepting Properties of Carbenes. *Angew. Chem., Int. Ed.* **2013**, *52*, 2939−2943. (b) Vummaleti, S. V. C.; Nelson, D. J.; Poater, A.; Gómez-Suárez, A.; Cordes, D. B.; Slawin, A. M. Z.; Nolan, S. P.; Cavallo, L. What can NMR spectroscopy of selenoureas and phosphinidenes teach us about the π-accepting abilities of *N*-heterocyclic carbenes? *Chem. Sci.* **2015**, *6*, 1895−1904. (c) Jacobsen, H.; Correa, A.; Poater, A.; Costabile, C.; Cavallo, L. Understanding the M−(NHC) (NHC = N-heterocyclic carbene) bond. *Coord. Chem. Rev.* **2009**, *253*, 687−703.

(8) Abbotto, A.; Bradamante, S.; Pagani, G. A. Pyridoneimines and Pyridonemethides: Substituent- and Solvent-Tunable Intramolecular Charge Transfer and Geometric Isomerism. *J. Org. Chem.* **2001**, *66*, 8883−8892.

(9) For PYE, see: (a) Doster, M. E.; Johnson, S. A. Selective C=F Bond Activation of Tetrafluorobenzenes by Nickel(0) with a Nitrogen Donor Analogous to N-Heterocyclic Carbenes. *Angew. Chem., Int. Ed.* **2009**, *48*, 2185−2187. (b) Shi, Q.; Thatcher, R. J.; Slattery, J.; Sauari, P. S.; Whitwood, A. C.; McGowan, P. C.; Douthwaite, R. E. Synthesis, Coordination Chemistry and Bonding of Strong N-Donor Ligands Incorporating the 1*H*-Pyridin-(2*E*)-Ylidene (PYE) Motif. *Chem. - Eur. J.* **2009**, *15*, 11346−11360. (c) Slattery, J.; Thatcher, R. J.; Shi, Q.; Douthwaite, R. E. Comparison of donor properties of *N*-heterocyclic carbenes and *N*-donors containing the 1*H*-pyridin-(2*E*)-ylidene motif. *Pure Appl. Chem.* **2010**, *82*, 1663−1671. (d) Thatcher, R. J.; Johnson, D. G.; Slattery, J. M.; Douthwaite, R. E. Charged Behaviour from Neutral Ligands: Synthesis and Properties of N-Heterocyclic Pseudo-amides. *Chem. - Eur. J.* **2012**, *18*, 4329−4336. For PYA, see: (e) Boyd, P. D. W.; Wright, L. J.; Zafar, M. N. Extending the Range of Neutral N-Donor Ligands Available for Metal Catalysts: *N*-[1-Alkylpyridin-4(1*H*)-ylidene]amides in Palladium-Catalyzed Cross-Coupling Reactions. *Inorg. Chem.* **2011**, *50*, 10522−10524. (f) Muller, C. M. A.; Babak, M. V.; Kubanik, M.; Hanif, M.; Jamieson, S. M. F.; Hartinger, C. G.; Wright, L. J. Pt(II) pyridinium amidate (PYA) complexes: Preparation and in vitro anticancer activity studies. *Inorg. Chim. Acta* **2016**, *450*, 124−130.

(10) (a) Donnelly, K. F.; Segarra, C.; Shao, L.-X.; Suen, R.; Müller-Bunz, H.; Albrecht, M. Adaptive N-Mesoionic Ligands Anchored to a Triazolylidene for Ruthenium-Mediated (De)Hydrogenation Catalysis. *Organometallics* **2015**, *34*, 4076−4084. (b) Navarro, M.; Li, M.; Müller-Bunz, H.; Bernhard, S.; Albrecht, M. Donor-Flexible Nitrogen Ligands for Efficient Iridium-Catalyzed Water Oxidation Catalysis. *Chem. - Eur. J.* **2016**, *22*, 6740−6745.

(11) (a) Doster, M. E.; Hatnean, J. A.; Jeftic, T.; Modi, S.; Johnson, S. A. Catalytic C−H Bond Stannylation: A New Regioselective Pathway to C−Sn Bonds via C−H Bond Functionalization. *J. Am. Chem. Soc.* **2010**, *132*, 11923−11925. (b) Doster, M. E.; Johnson, S. A. Carbon−Hydrogen Bond Stannylation and Alkylation Catalyzed by Nitrogen-Donor-Supported Nickel Complexes: Intermediates with Ni−Sn

DOI: 10.1021/acs.inorgchem.7b01654
Inorg. Chem. XXXX, XXX, XXX−XXX

Bonds and Catalytic Carbostannylation of Ethylene with Organostannanes. *Organometallics* **2013**, *32*, 4174−4184.
(12) Leigh, V.; Carleton, D. J.; Olguin, J.; Mueller-Bunz, H.; Wright, L. J.; Albrecht, M. Solvent-Dependent Switch of Ligand Donor Ability and Catalytic Activity of Ruthenium(II) Complexes Containing Pyridinylidene Amide (PYA) N-Heterocyclic Carbene Hybrid Ligands. *Inorg. Chem.* **2014**, *53*, 8054−8060.
(13) Lundgren, R. J.; Stradiotto, M. *Ligand Design in Metal Chemistry: Reactivity and Catalysis*; John Wiley & Sons: Chichester, U.K., 2016.
(14) Robert-Piessard, S.; Le Baut, G.; Courant, J.; Brion, J. D.; Sparfel, L.; Bouhayat, S.; Petit, J. Y.; Sanchez, R. Y.; Juge, M.; Grimaud, N.; Welin, L. Non-acidic anti-inflammatory compounds: activity of N-(4,6-dimethyl-2-pyridinyl) benzamides and derivatives. *Eur. J. Med. Chem.* **1990**, *25*, 9−19.
(15) (a) Davies, D. L.; Donald, S. M. A.; Macgregor, S. A. Computational Study of the Mechanism of Cyclometalation by Palladium Acetate. *J. Am. Chem. Soc.* **2005**, *127*, 13754−13755. (b) Davies, D. L.; Donald, S. M. A.; Al-Duaij, O.; Fawcett, J.; Little, C.; Macgregor, S. A. N−H versus C−H Activation of a Pyrrole Imine at {Cp*Ir}: A Computational and Experimental Study. *Organometallics* **2006**, *25*, 5976−5978. (c) Albrecht, M. Cyclometalation Using d-Block Transition Metals: Fundamental Aspects and Recent Trends. *Chem. Rev.* **2010**, *110*, 576−623.
(16) While the pyridylidene protons for the nonsubstituted complex **4a** and the substituted iridium complexes **4c**−**4e** are similar (δ_H 7.53−7.57 for H_α and 8.42−8.47 for H_β), these signals are significantly upfield-shifted in complex **4b** (7.46 and 8.27 ppm, respectively). This shift is presumably due to the ortho-positioned methoxy group in complex **4b** and the ensuing repulsion of the syn arrangement of the methoxy and carbonyl groups.
(17) (a) Mishra, A.; Kaushik, N. K.; Verma, A. K.; Gupta, R. Synthesis, characterization and antibacterial activity of cobalt(III) complexes with pyridine−amide ligands. *Eur. J. Med. Chem.* **2008**, *43*, 2189−2196. (b) Kumar, P.; Gupta, R. The wonderful world of pyridine-2,6-dicarboxamide based scaffolds. *Dalton Trans.* **2016**, *45*, 18769−18733.
(18) (a) Zassinovich, G.; Mestroni, G.; Gladiali, S. Asymmetric hydrogen transfer reactions promoted by homogeneous transition metal catalyst. *Chem. Rev.* **1992**, *92*, 1051−1069. (b) Klomp, D.; Hanefeld, U.; Peters, J. A. In *The Handbook of Homogeneous Hydrogenation*; de Vries, J. G., Elsevier, C. J., Eds.; Wiley-VCH: Weinheim, Germany, 2007; p 585. (c) Samec, J. S. M.; Bäckvall, J.-E.; Andersson, P. G.; Brandt, P. Mechanistic aspects of transition metal-catalyzed hydrogen transfer reactions. *Chem. Soc. Rev.* **2006**, *35*, 237−248. (d) Wang, D.; Astruc, D. The Golden Age of Transfer Hydrogenation. *Chem. Rev.* **2015**, *115*, 6621−6686. (e) Wang, C.; Pettman, A.; Basca, J.; Xiao, J. A Versatile Catalyst for Reductive Amination by Transfer Hydrogenation. *Angew. Chem., Int. Ed.* **2010**, *49*, 7548−7552. (f) Talwar, D.; Wu, X.; Saidi, O.; Salguero, N. P.; Xiao, J. Versatile Iridicyle Catalyst for Highly Efficient and Chemoselecive Transfer Hydrogenation of Carbonyl Compounds in Water. *Chem. - Eur. J.* **2014**, *20*, 12835−12842. (g) Wei, Y.; Xue, D.; Lei, Q.; Wang, C.; Xiao, J. Cyclometalated Iridium Complexes for Transfer Hydrogenation of Carbonyl Groups in Water. *Green Chem.* **2013**, *15*, 629−634.
(19) While this improvement of the catalytic activity is substantial, it should be noted that many iridium(III) complexes are much more active in transfer hydrogenation, and TOFs in excess of 1000 h^{-1} are not uncommon. For example see: (a) Gülcemal, S.; Gökce, A. G.; Çetinkaya, B. N-Benzyl Substituted N-Heterocyclic Carbene Complexes of Iridium(I): Assessment in Transfer Hydrogenation Catalyst. *Inorg. Chem.* **2013**, *52*, 10601−10609. (b) Jiménez, M. V.; Fernández-Tornos, J.; Pérez-Torrente, J. J.; Modrego, F. J.; García-Orduna, P.; Oro, L. A. Mechanistic Insights into Transfer Hydrogenation Catalysis by $[Ir(cod)(NHC)_2]^+$ Complexes with Functionalized N-Heterocyclic Carbene Ligands. *Organometallics* **2015**, *34*, 926−940. (c) Gülcemal, S.; Gökce, A. G.; Çetinkaya, B. Iridium(I) NHeterocyclic Carbene Complexes of Benzimidazol-2-ylidene: Effect of Electron Donating Groups on the Catalytic Transfer Hydrogenation Reaction. *Dalton Trans.* **2013**, *42*, 7305−7311. (d) Gülcemal, D.; Gökce, A. G.; Gülcemal, S.; Cetinkaya, B. Hydroxyl and Ester Functionalized N-Heterocyclic Carbene Complexes of Iridium(I): Efficient Catalysts for Transfer Hydrogenation Reactions. *RSC Adv.* **2014**, *4*, 26222−26230. (e) Zhu, X.-H.; Cai, L.-H.; Wang, C.-X.; Wang, Y.-N.; Guo, X.-Q.; Hou, X.-F. Efficient and Versatile Transfer Hydrogenation Catalysts: Iridium (III) and Ruthenium (II) Complexes with 4-Acetylbenzyl-NHeterocyclic Carbenes. *J. Mol. Catal. A: Chem.* **2014**, *393*, 134−141.
(20) While the addition of a third methoxy group may further lower the energy of the initially turnover-limiting step, it may have an opposite effect on another step on the catalytic cycle and hence shift the turnover-limiting transformation. However, it would be most remarkable if such a shift results in the dramatic loss of the catalytic activity as observed with **4e** compared to **4d**.
(21) Chien, S. L.; Adams, R. Stereochemistry of Diphenyls. XXXV.[1] The Effect of 3′ Substituents on the Rate of Racemization of 2-Nitro-6-carboxy-2′-methoxydiphenyl. *J. Am. Chem. Soc.* **1934**, *56*, 1787−1792. (b) Brown, J. M.; Pearson, M.; Jastrzebski, J. T. B. H.; van Koten, G. Intramolecular Facilitation of aryl-transfer from tin in palladium-catalysed cross-coupling. *J. Chem. Soc., Chem. Commun.* **1992**, 1440−1441.
(22) (a) Delgado-Rebollo, M.; Canseco-Gonzalez, D.; Hollering, M.; Mueller-Bunz, H.; Albrecht, M. Synthesis and catalytic alcohol oxidation and ketone transfer hydrogenation activity of donor-functionalized mesoionic triazolylidene ruthenium(II) complexes. *Dalton Trans.* **2014**, *43*, 4462−4473. (b) Farrell, K.; Müller-Bunz, H.; Albrecht, M. Synthesis, Isomerization, and Catalytic Transfer Hydrogenation Activity of Rhodium(III) Complexes Containing Both Chelating Dicarbenes and Diphosphine Ligands. *Organometallics* **2015**, *34*, 5723−5733.
(23) Albrecht, M.; Miecznikowski, J. R.; Samuel, A.; Faller, J. W.; Crabtree, R. H. Chelated Iridium(III) Bis-carbene Complexes as Air-Stable Catalysts for Transfer Hydrogenation. *Organometallics* **2002**, *21*, 3596−3604.
(24) (a) Pàmies, O.; Bäckvall, J.-E. Studies on the Mechanism of Metal-Catalyzed Hydrogen Transfer from Alcohols to Ketones. *Chem. - Eur. J.* **2001**, *7*, 5052−5058. (b) Clapham, S. E.; Hadzovic, A.; Morris, R. H. Mechanisms of the H_2-hydrogenation and transfer hydrogenation of polar bonds catalyzed by ruthenium hydride complexes. *Coord. Chem. Rev.* **2004**, *248*, 2201−2237.
(25) (a) Casey, C. P.; Singer, S. W.; Powell, D. R.; Hayashi, R. K.; Kavana, M. Hydrogen Transfer to Carbonyls and Imines from a Hydroxycyclopentadienyl Ruthenium Hydride: Evidence for Concerted Hydride and Proton Transfer. *J. Am. Chem. Soc.* **2001**, *123*, 1090−1110. (b) Han, J.; Kang, S.; Lee, H.-K. Dynamic kinetic resolution in the stereoselective synthesis of 4,5-diaryl cyclic sulfamidates by using chiral rhodium-catalyzed asymmetric transfer hydrogenation. *Chem. Commun.* **2011**, *47*, 4004−4006. (c) Iturmendi, A.; García, N.; Jaseer, E. A.; Munárriz, J.; Sanz Miguel, P. J.; Polo, V.; Iglesias, M.; Oro, L. A. N-Heterocyclic olefins as ancillary ligands in catalysis: a study of their behaviour in transfer hydrogenation reactions. *Dalton Trans.* **2016**, *45*, 12835−12845. (d) Mai, V. H.; Nikonov, G. I. Transfer Hydrogenation of Nitriles, Olefins, and *N*-Heterocycles Catalyzed by an *N*-Heterocyclic Carbene-Supported Half-Sandwich Complex of Ruthenium. *Organometallics* **2016**, *35*, 943−949. (e) Xu, C.; Zhang, L.; Dong, C.; Xu, J.; Pan, Y.; Li, Y.; Zhang, H.; Li, H.; Yu, Z.; Xu, L. Iridium-Catalyzed Transfer Hydrogenation of 1,10-Phenanthrolines Using Formic Acid as the Hydrogen Source. *Adv. Synth. Catal.* **2016**, *358*, 567−572. (f) Li, Y.; Lei, M.; Yuan, W.; Meggers, E.; Gong, L. An N-Heterocylcic Carbene Iridium Catalyst with Metal-centered Chirality for Enantioselective Transfer Hydrogenation of Imines. *Chem. Commun.* **2017**, *53*, 8089−8092. (g) Wang, D.-W.; Wang, D.-S.; Chen, Q.-A.; Zhou, Y.-G. Asymmetric Hydrogenation with Water/Silane as the Hydrogen Source. *Chem. - Eur. J.* **2010**, *16*, 1133−1136. (h) Chen, H.-Y.; Wang, C.; Wu, X.; Jiang, X.; Catlow, C. R. A.; Xiao, J. Iridicycle-Catalysed Imine Reduction: An Experimental and Computational Study of the Mechanism. *Chem. - Eur. J.* **2015**, *21*, 16564−16577. (i) Foubelo, F.; Yus, M. Catalytic Asymmetric Transfer Hydrogenation

DOI: 10.1021/acs.inorgchem.7b01654
Inorg. Chem. XXXX, XXX, XXX−XXX

of Imines: Recent Advances. *Chem. Rec.* **2015**, *15*, 907−924. Stirling, M. J.; Sweeney, G.; MacRory, K.; Blacker, A. J.; Page, M. J. The kinetics and mechanism of the organo-iridium-catalysed enantioselective reduction of imines. *Org. Biomol. Chem.* **2016**, *14*, 3614−3622.
(26) Cannizzaro, S. Ueber den der Benzoësäure entsprechenden Alkohol. *Justus Liebigs Ann. Chem.* **1853**, *88*, 129−130.
(27) Morris, S. A.; Gusev, D. G. Rethinking the Claisen-Tishchenko Reaction. *Angew. Chem., Int. Ed.* **2017**, *56*, 6228−6231.
(28) (a) Ohkuma, T.; Koizumi, M.; Muñiz, K.; Hilt, G.; Kabuto, C.; Noyori, R. *trans*-RuH(η^1-BH_4)(binap)(1,2-diamine): A Catalyst for Asymmetric Hydrogenation of Simple Ketones under Base-Free Conditions. *J. Am. Chem. Soc.* **2002**, *124*, 6508−6509. (b) Abdur-Rashid, K.; Clapham, S. E.; Hadzovic, A.; Harvey, J. N.; Lough, A. J.; Morris, R. H. Mechanism of the Hydrogenation of Ketones Catalyzed by *trans*-Dihydrido(diamine)ruthenium(II) Complexes. *J. Am. Chem. Soc.* **2002**, *124*, 15104−15118. (c) Dong, Z.-R.; Li, Y.-Y.; Chen, J.-S.; Li, B.-Z.; Xing, Y.; Gao, J.-X. Highly Efficient Iridium Catalyst for Asymmetric Transfer Hydrogenation of Aromatic Ketones under Base-Free Conditions. *Org. Lett.* **2005**, *7*, 1043−1045. (d) Esteruelas, M. A.; García-Yebra, C.; Oñate, E. [$H(EtOH)_2$][{$OsCl(\eta^4$-COD)}$_2$(μ-H)(μ-$Cl)_2$] as an Intermediate for the Preparation of [$OsCl_2$(COD)]$_x$ and Its Activity as an Ionic Hydrogenation and Etherification Catalyst. *Organometallics* **2008**, *27*, 3029−3036. (e) Carrión, M. C.; Sepúlveda, F.; Jalón, F. A.; Manzano, B. R.; Rodríguez, A. M. Base-Free Transfer Hydrogenation of Ketones Using Arene Ruthenium(II) Complexes. *Organometallics* **2009**, *28*, 3822−3833. (f) Ruff, A.; Kirby, C.; Chan, B. C.; O'Connor, A. R. Base-Free Transfer Hydrogenation of Ketones Using Cp*Ir(pyridinesulfonamide)Cl Precatalyst. *Organometallics* **2016**, *35*, 327−335. (g) Corberán, R.; Peris, E. An Unusual Example of Base-Free Catalyzed Reduction of C═O and C═NR Bonds by Transfer Hydrogenation and Some Useful Implications. *Organometallics* **2008**, *27*, 1954−1958.
(29) (a) Marciniec, B. In *Applied Homogeneous Catalysis with Organometallic Compounds*; Cornils, B., Herrmann, W. A., Eds.; Wiley-VCH: Weinheim, Germany, 2002; Vol. *1*. (b) Marciniec, B. In *Hydrosilylation: A Comprehensive Review on Recent Advances*; Matisons, J., Ed.; Springer: New York, 2009; pp 53−123.
(30) For example, see: (a) Elschenbroich, C. *Organometallics*; Wiley-VCH: Weinheim, Germany, 2006. (b) Speier, J. L. Homogeneous Catalysis of Hydrosilation by Transition Metals. *Adv. Organomet. Chem.* **1979**, *17*, 407−447. (c) Karstedt, B. D. U.S. Patent 3,775,452, 1973.
(31) For example, see: (a) Trost, B. M.; Ball, Z. T. Markovnikov Alkyne Hydrosilylation Catalyzed by Ruthenium Complexes. *J. Am. Chem. Soc.* **2001**, *123*, 12726−12727. (b) Trost, B. M.; Ball, Z. T. Intramolecular Endo-Dig Hydrosilylation Catalyzed by Ruthenium: Evidence for a New Mechanistic Pathway. *J. Am. Chem. Soc.* **2003**, *125*, 30−31. (c) Chung, L. W.; Wu, Y.-D.; Trost, B. M.; Ball, Z. T. A Theoretical Study on the Mechanism, Regiochemistry, and Stereochemistry of Hydrosilylation Catalyzed by Cationic Ruthenium Complexes. *J. Am. Chem. Soc.* **2003**, *125*, 11578−11582. (d) Dragutan, V.; Dragutan, I.; Delaude, L.; Demonceau, A. NHC−Ru complexes—Friendly catalytic tools for manifold chemical transformations. *Coord. Chem. Rev.* **2007**, *251*, 765−794. (e) Maifeld, S. V.; Tran, M. N.; Lee, D. Hydrosilylation of alkynes catalyzed by ruthenium carbene complexes. *Tetrahedron Lett.* **2005**, *46*, 105−108. (f) Martín, M.; Sola, E.; Lahoz, F. J.; Oro, L. A. Trans Additions of Silanes to 1-Alkynes Catalyzed by Ruthenium Complexes: Role of in Situ Formed Polynuclear Aggregates. *Organometallics* **2002**, *21*, 4027−4029. (g) Gao, R.; Pahls, D. R.; Cundari, T. R.; Yi, C. S. Experimental and Computational Studies of the Ruthenium-Catalyzed Hydrosilylation of Alkynes: Mechanistic Insights into the Regio- and Stereoselective Formation of Vinylsilanes. *Organometallics* **2014**, *33*, 6937−6944.
(32) For example, see: (a) Jiménez, M. V.; Pérez-Torrente, J. J.; Bartolomé, M. I.; Gierz, V.; Lahoz, F. J.; Oro, L. A. Rhodium(I) Complexes with Hemilabile N-Heterocyclic Carbenes: Efficient Alkyne Hydrosilylation Catalysts. *Organometallics* **2008**, *27*, 224−234. (b) Ojima, I.; Clos, N.; Donovan, R. J.; Ingallina, P. Hydrosilylation of 1-hexyne catalyzed by rhodium and cobalt-rhodium mixed-metal complexes. Mechanism of apparent trans addition. *Organometallics* **1990**, *9*, 3127−3133. (c) Poyatos, M.; Mas-Marzá, E.; Mata, J. A.; Sanaú, M.; Peris, E. Synthesis, Reactivity, Crystal Structures and Catalytic Activity of New Chelating Bisimidazolium-Carbene Complexes of Rh. *Eur. J. Inorg. Chem.* **2003**, *2003*, 1215−1221. (d) Busetto, L.; Cassani, M. C.; Femoni, C.; Mancinelli, M.; Mazzanti, A.; Mazzoni, R.; Solinas, G. N-Heterocyclic Carbene-Amide Rhodium(I) Complexes: Structures, Dynamics, and Catalysis. *Organometallics* **2011**, *30*, 5258−5272. (e) Tanke, R. S.; Crabtree, R. H. Unusual activity and selectivity in alkyne hydrosilylation with an iridium catalyst stabilized by an oxygen-donor ligand. *J. Am. Chem. Soc.* **1990**, *112*, 7984−7989. (f) Mas-Marzá, E.; Poyatos, M.; Sanaú, M.; Peris, E. Carbene Complexes of Rhodium and Iridium from Tripodal N-Heterocyclic Carbene Ligands: Synthesis and Catalytic Properties. *Inorg. Chem.* **2004**, *43*, 2213−2219. (g) Mas-Marzá, E.; Sanaú, M.; Peris, E. *Inorg. Chem.* **2005**, *44*, 9961−9967. (h) Zanardi, A.; Peris, E.; Mata, J. A. Alkenyl-functionalized NHC iridium-based catalysts for hydrosilylation. *New J. Chem.* **2008**, *32*, 120−126. (i) Viciano, M.; Mas-Marzá, E.; Sanaú, M.; Peris, E. Synthesis and Reactivity of New Complexes of Rhodium and Iridium with Bis-(dichloroimidazolylidene) Ligands. Electronic and Catalytic Implications of the Introduction of the Chloro Substituents in the NHC Rings. *Organometallics* **2006**, *25*, 3063−3069. (j) Vicent, C.; Viciano, M.; Mas-Marzá, E.; Sanaú, M.; Peris, E. Electrospray Ionization Mass Spectrometry Studies on the Mechanism of Hydrosilylation of Terminal Alkynes Using an N-Heterocyclic Carbene Complex of Iridium, Allow Detection/Characterization of All Reaction Intermediates. *Organometallics* **2006**, *25*, 3713−3720.
(33) For example, see: (a) Esteruelas, M. A.; Lahoz, F. J.; Oñate, E.; Oro, L. A.; Rodríguez, L. Reactions of Ir(acac)(cyclooctene)(PCy_3) with H_2, HC⋮CR, $HSiR_3$, and $HSnPh_3$: The Acetylacetonato Ligand as a Stabilizer for Iridium(I), Iridium(III), and Iridium(V) Derivatives. *Organometallics* **1996**, *15*, 823−834. (b) Iglesias, M.; Sanz Miguel, P. J.; Polo, V.; Fernández-Alvarez, F.; Pérez-Torrente, J. J.; Oro, L. A. An Alternative Mechanistic Paradigm for the β-*Z* Hydrosilylation of Terminal Alkynes: The Role of Acetone as a Silane Shuttle. *Chem. - Eur. J.* **2013**, *19*, 17559−17566. (c) Pérez-Torrente, J.; Nguyen, D. H.; Jiménez, M. V.; Modrego, F. J.; Puerta-Oteo, R.; Gómez-Bautista, D.; Iglesias, M.; Oro, L. A. Hydrosilylation of Terminal Alkynes Catalyzed by a ONO-Pincer Iridium(III) Hydride Compound: Mechanistic Insights into the Hydrosilylation and Dehydrogenative Silylation Catalysis. *Organometallics* **2016**, *35*, 2410−2422. (d) Corre, Y.; Werlé, C.; Brelot-Karmazin, L.; Djukic, J.-P.; Agbossou-Niedercorn, F.; Michon, C. Regioselective hydrosilylation of terminal alkynes using pentamethylcyclopentadienyl iridium(III) metallacycle catalysts. *J. Mol. Catal. A: Chem.* **2016**, *423*, 256−263. (e) Iglesias, M.; Pérez-Nicolás, M.; Miguel, P. J. S.; Polo, V.; Fernández-Alvarez, F. J.; Pérez-Torrente, J. J.; Oro, L. A. A synthon for a 14-electron Ir(III) species: catalyst for highly selective β-(*Z*) hydrosilylation of terminal alkynes. *Chem. Commun.* **2012**, *48*, 9480−9482.
(34) For β(*E*) isomer selectivity, see: (a) Hesp, K. D.; Wechsler, D.; Cipot, J.; Myers, A.; McDonald, R.; Ferguson, M. J.; Schatte, G.; Stradiotto, M. Exploring the Utility of Neutral Rhodium and Iridium κ^2-P,O and κ^2-P(S),O Complexes as Catalyst for Alkene Hydrogenation and Hydrosilylation. *Organometallics* **2007**, *26*, 5430−5437. (b) Cipot; McDonald, R.; Ferguson, M. J.; Schatte, G.; Stradiotto, M. Cationic and Formally Zwitterionic Rhodium(I) and Iridium(I) Derivatives of a P,N-Substituted Indene: A Comparative Synthetic, Structural, and Catalytic Investigation. *Organometallics* **2007**, *26*, 594−608.
(35) Sridevi, V. S.; Fan, W. Y.; Leong, W. K. Stereoselective Hydrosilylation of Terminal Alkynes Catalyzed by [$Cp^*IrCl_2]_2$: A Computational and Experimental Study. *Organometallics* **2007**, *26*, 1157−1160.
(36) Ball, R. G.; Graham, W. A. G.; Heinekey, D. M.; Hoyano, J. K.; McMaster, A. D.; Mattson, B. M.; Michel, S. T. Synthesis and structure of dicarbonylbis(.eta.-pentamethylcyclopentadienyl)diiridium. *Inorg. Chem.* **1990**, *29*, 2023−2025.

DOI: 10.1021/acs.inorgchem.7b01654
Inorg. Chem. XXXX, XXX, XXX−XXX

(37) Macchi, P.; Bürgi, H. B.; Chimpri, A. S.; Hauser, J.; Gal, Z. Low-energy contamination of Mo microsource X-ray radiation: analysis and solution of the problem. *J. Appl. Crystallogr.* **2011**, *44*, 763−771.
(38) *CrysAlisPro*, version 1.171.34.44; Oxford Diffraction Ltd.: Yarnton, Oxfordshire, U.K., 2010.
(39) Sheldrick, G. M. SHELXT − Integrated space-group and crystal structure determination. *Acta Crystallogr., Sect. A: Found. Adv.* **2015**, *71*, 3−8.

DOI: 10.1021/acs.inorgchem.7b01654
Inorg. Chem. XXXX, XXX, XXX−XXX